symmetry

MDPI

Article

Uncovering Symmetric and Asymmetric Deterioration Patterns in Maryland's Steel Bridges Through Time-Series Clustering and Principal Component Analysis

Soroush Piri [1,*], Zeinab Bandpey [2], Mehdi Shokouhian [2] and Ruel Sabellano [2,3]

[1] Department of Architecture, Urbanism, and Built Environments, School of Architecture and Planning, Morgan State University, Baltimore, MD 21251, USA
[2] Department of Civil Engineering, Morgan State University, Baltimore, MD 21251, USA; zeinab.bandpey@morgan.edu (Z.B.); mehdi.shokouhian@morgan.edu (M.S.); rusab1@morgan.edu or rsabellano@mdta.state.md.us (R.S.)
[3] Maryland Transportation Authority (MDTA), Baltimore, MD 21222, USA
* Correspondence: soroush.piri@morgan.edu

Abstract

This study analyzes long-term deterioration patterns in 1378 Maryland steel bridges using annual Bridge Health Index (BHI) records from 1995–2021. Missing observations were addressed through linear interpolation combined with forward/backward filling, after which feature-wise z-score standardization was applied to ensure comparability across annual trajectories. Euclidean K-means clustering (k-means++ initialization, 10 restarts) was implemented to identify deterioration archetypes, with K = 6 selected using the elbow method and the silhouette coefficient. Cluster-internal stability was evaluated using bridge-level Root Mean Squared Error (RMSE), and uncertainty in median deterioration profiles was quantified using 2000-iteration percentile-based bootstrap confidence intervals. To interpret structural and contextual drivers within each group, Principal Component Analysis (PCA) was performed on screened and standardized geometric, structural, and traffic-related attributes. Results revealed strong imbalance in cluster membership (757, 503, 35, 33, 44, and 6 bridges), reflecting substantial diversity in long-term BHI behavior. Cluster-median RMSE values ranged from 2.69 to 22.66, while wide confidence bands in smaller clusters highlighted elevated uncertainty due to limited sample size. PCA indicated that span length, deck width, truck percentage, and projected future ADT were the most influential differentiators of deteriorating clusters, while stable clusters were distinguished by consistently high BHI component values and limited geometric complexity. Missing rehabilitation records prevented definitive attribution of U-shaped or recovering trajectories to specific intervention events. Overall, this study establishes a scalable, statistically supported framework for deterioration-trajectory profiling and provides actionable insight for proactive inspection scheduling, rehabilitation prioritization, and long-term asset management planning for state-level bridge networks.

Keywords: Bridge Health Index (BHI); steel bridge deterioration; time-series clustering; Principal Component Analysis (PCA); predictive asset management; unsupervised learning

check for updates

Academic Editor: Wang Chen

Received: 30 October 2025
Revised: 26 November 2025
Accepted: 29 November 2025
Published: 3 December 2025

Citation: Piri, S.; Bandpey, Z.; Shokouhian, M.; Sabellano, R. Uncovering Symmetric and Asymmetric Deterioration Patterns in Maryland's Steel Bridges Through Time-Series Clustering and Principal Component Analysis. *Symmetry* **2025**, *17*, 2074. https://doi.org/10.3390/sym17122074

Correction Statement: This article has been republished with a minor change. The change does not affect the scientific content of the article and further details are available within the backmatter of the website version of this article.

Copyright: © 2025 by the authors. Licensee MDPI, Basel, Switzerland. This article is an open access article distributed under the terms and conditions of the Creative Commons Attribution (CC BY) license (https://creativecommons.org/licenses/by/4.0/).

1. Introduction

Transportation infrastructure plays a central role in regional mobility and economic performance. In the United States, more than 623,000 bridges support critical traffic networks, yet many are operating beyond their intended service life, with approximately 6.8%

in poor condition [1–3]. Bridge inspection remains heavily dependent on biennial visual assessments, which are resource-intensive and limited in their ability to detect gradual or nonlinear deterioration [4–7]. Maryland faces similar challenges, with 278 structures currently classified as poor or structurally deficient [8,9]. Steel bridges constitute a particularly critical subset due to their exposure to corrosion, fatigue loading, and high freight volumes [10,11].

Recent advances in civil infrastructure analytics highlight the potential of data-driven and machine-learning methods to improve deterioration prediction and support asset management [12]. To this end, the present study analyzes agency-provided Bridge Health Index (BHI) time-series data for 1378 steel bridges across Maryland (1995–2021), compiled from the Maryland Department of Transportation and Maryland Transportation Authority records. Supporting structural, traffic, and climatic attributes were sourced from the FHWA National Bridge Inventory, MDOT-SHA, and NOAA environmental records, enabling contextual interpretation of deterioration behavior across the statewide network.

Despite progress in deterioration modeling, there remains a lack of network-scale studies leveraging continuous BHI time series to identify interpretable deterioration archetypes. Existing studies generally rely on discrete condition ratings, short monitoring windows, or component-level prediction models, limiting their ability to capture nonlinear performance trajectories across large bridge inventories. To address this gap, this study develops a reproducible analytical pipeline combining hybrid imputation, z-score normalization, K-means clustering, bootstrap uncertainty quantification, and PCA-based structural interpretation.

1.1. Traditional Deterioration & BMS Approaches

Conventional deterioration modeling frameworks including Markov chains, regression-based forecasting, and survival analysis remain central to many Bridge Management Systems (BMS) [13–17]. However, recent studies have shown systematic bias and limited sensitivity to nonlinear deterioration behavior, even when enhanced with probabilistic methods [18–21].

1.2. Unsupervised Clustering & Time-Series Pattern Discovery

More recently, advances in data-driven analytics and machine learning have expanded the toolkit for infrastructure deterioration prediction, offering greater flexibility in modeling nonlinear degradation patterns and integrating large datasets. As highlighted in a comprehensive review by [22], shows that traditional Markov, regression, and survival models cannot capture gradual or nonlinear deterioration or reveal system-wide patterns. Recent work shows that explainable deep learning can extract insights from raw time-series data. The DLUHS framework [23], for instance, uses CNNs to predict uniform hazard spectra from seismic waveforms without manual feature engineering. Recent studies show that deep learning can extract deterioration patterns from time-series data to support bridge condition evaluation. This transition toward continuous monitoring and machine-learning analytics aligns with emerging data-driven asset management frameworks [24,25].

However, most deep learning work remains focused on event- or component-level data, whereas network-scale deterioration requires comparing long-term trajectories. Recent SHM studies show that unsupervised learning using clustering and dimensionality reduction can reveal hidden deterioration patterns across large systems [26]. The unsupervised learning approach can reveal hidden deterioration patterns without requiring predefined labels, helping identify bridges needing targeted maintenance [27,28].

This approach supports network-wide pattern discovery, abnormal behavior detection, and integration into Bridge Management Systems through standardized data preparation. Recent studies have applied unsupervised learning techniques particularly K-means clus-

tering and PCA to analyze bridge performance at scale. Clustering helps identify groups of bridges with shared deterioration behavior; for example, Landi (2025) used a Weibull Mixture Model-based SNOB algorithm to cluster NBI sojourn times into "fragile," "normal," and "robust" aging groups [29]. Their semi-Markov modeling showed that clustered groups better represent network-level deterioration than a single undifferentiated model. Similarly, Chang and Chi (2019) used K-means clustering on 1944 bridges in Korea and found clear differences in damage frequency across clusters, with predictive accuracy improving markedly after clustering (AUC rising from 0.655 to 0.745) [30] Masiero (2024) used GMM and DBSCAN to cluster GNSS vibration time-series from the Valgadena viaduct in Italy [24], revealing persistent structural modes and improving real-time anomaly detection under diverse operational conditions.

1.3. PCA for Interpretability of Deterioration Trends

While clustering effectively reveals groups of structurally similar bridges with shared deterioration patterns, Principal Component Analysis (PCA) complements this by uncovering the key features such as age, span length, and traffic volume that drive variation in condition trends across the network [31–34]. The PCA method eliminates redundant information between deck and superstructure ratings which show strong correlation while it reveals hidden deterioration patterns that standard condition ratings cannot detect. The method generates orthogonal axes which improve clustering results and provide better interpretability of the results [35–41]. Sen (2019) demonstrated the value of PCA for structural health monitoring by applying it to vibration sensor data from continuous beam bridges to separate damage-related changes from environmental effects such as temperature [42]. Their results showed clear discontinuities in principal components at the onset of structural damage, enabling accurate quantification and tracking of deterioration. Similarly, Yuan (2024) applied PCA using a moving temporal window to detect anomalies in vibration data under varying traffic and environmental conditions [43]. Their approach reduced dimensionality, suppressed noise, and highlighted deterioration-relevant modes, enabling scalable, real-time damage detection across bridge networks. Another regional study in Hebei, China [40] applied a data-driven framework across thousands of bridges by integrating inspection histories with structural attributes. PCA was used to extract latent features such as span length, deck age, and traffic volume that govern deterioration trends, and these were subsequently used to support forecasting models and guide maintenance prioritization at a network scale.

In the broader context of infrastructure performance, understanding deterioration also requires distinguishing between symmetric and asymmetric behaviors across bridge networks [44,45]. Symmetric deterioration describes consistent and uniform degradation trends that occur among structurally or functionally similar bridges [46], while asymmetric deterioration represents irregular, localized deviations influenced by site-specific or environmental conditions [47]. Recognizing both forms provides a balanced view of system behavior, helping agencies identify whether performance changes stem from network-wide patterns or isolated anomalies.

The Bridge Health Index (BHI) serves as a standard measurement tool for bridge assessment in transportation networks according to [48,49]. The BHI system generates a single continuous score which combines structural element conditions with service performance metrics to help agencies measure bridge health levels. Multiple state transportation agencies including the Maryland Transportation Authority (MDTA) use BHI frameworks like the modified Denver Bridge Health Index (DBHI) to monitor bridge conditions and determine maintenance priorities and resource distribution. The research uses BHI time-series data from Maryland agencies including MDTA to analyze steel bridge deterioration

patterns throughout the state. The National Bridge Inventory (NBI) system determines bridge condition ratings through the lowest score from deck and super-structure and sub-structure components [50], which can hide both network-wide performance patterns and system-wide information. The NBI system experiences problems with data quality and consistency because different evaluation studies have found various errors and missing information which results in incorrect network-level and large-scale analysis results [51]. The BHI system generates a single composite indicator which tracks all essential components' health status better than separate NBI ratings do because it enables network-wide monitoring and supports extended performance evaluation [52]. The decision-support framework developed by Karaaslan [53] combines nondestructive evaluation results with deterioration prediction models to create network-based bridge management and maintenance plans. The research demonstrates how BHI-type continuous composite indices support network-wide strategic planning through their ability to link structural condition data with strategic decision-making [53]. Researchers use Principal Component Analysis (PCA) as a dimensionality reduction method to understand BHI network trend variations better [54,55].

Despite growing interest in data-driven techniques, several limitations persist in the existing literature. Most clustering studies focus on structural health monitoring (SHM) sensor data or limited case studies [56,57]. Few have combined clustering and PCA to analyze long-term Bridge Health Index (BHI) trends across full statewide networks [24,57,58]. Additionally, existing studies rarely integrate contextual factors such as traffic demand, design load, or age when interpreting deterioration clusters [18]. This gap is particularly consequential for steel bridges, which represent a major share of Maryland's inventory and face pronounced long-term maintenance challenges. While clustering and PCA have shown value individually, their combined application to statewide BHI time-series remains limited. To address this, the present study develops an interpretable framework that integrates time-series clustering with PCA, incorporating contextual bridge characteristics to reveal shared deterioration patterns and the key drivers behind them. This combined approach supports more informed maintenance planning and enhances network-level resilience.

To align with these gaps, this study makes four key contributions. First, it compiles, aligns, and standardizes multi-year BHI records for Maryland's statewide steel bridge network using a reproducible cleaning and imputation pipeline. Second, it derives interpretable deterioration archetypes using K-means clustering supported by bootstrap-based uncertainty quantification. Third, it employs Principal Component Analysis (PCA) to identify the structural, geometric, and operational features that differentiate deterioration groups. Fourth, it provides a scalable and transparent framework that transportation agencies can use to support proactive, data-informed maintenance planning across large bridge inventories. By explicitly quantifying symmetric and asymmetric deterioration behaviors using a Robinson-type Symmetry Index, this study contributes to the emerging discourse on symmetry and asymmetry in infrastructure performance.

The primary objectives of this study are to (1) identify network-level deterioration archetypes using agency-reported BHI time series; (2) quantify temporal uncertainty in cluster-level median trajectories using non-parametric bootstrap resampling; and (3) interpret the dominant structural, geometric, and traffic-related drivers of each deterioration pattern using cluster-specific PCA.

The remainder of this manuscript is organized as follows: Section 2 details the data sources, preprocessing procedures, and analytical workflow, including the clustering, bootstrap uncertainty estimation, and PCA-based feature interpretation. Section 3 presents the results for Maryland's steel bridges, including cluster characterization, symmetry quantification, uncertainty analysis, and principal component interpretation. Section 4 discusses

the findings, practical implications, and methodological limitations in the context of existing literature. Finally, Section 5 concludes the study and outlines directions for future research.

2. Materials and Methods

In this work we devise a data-driven framework aimed at teasing the long-term deterioration trends of Maryland's steel bridges on a scale. Our methodology integrates time-series clustering and dimensionality reduction, helping surface degradation behaviors and identifying the variables that most influence bridge health. By blending pattern recognition, with a feature analysis the framework delivers both network-wide insights and practical strategies, for predictive bridge maintenance. To provide a visual overview of the analytical stages undertaken in this research, a workflow diagram summarizing the major methodological steps is presented in Figure 1.

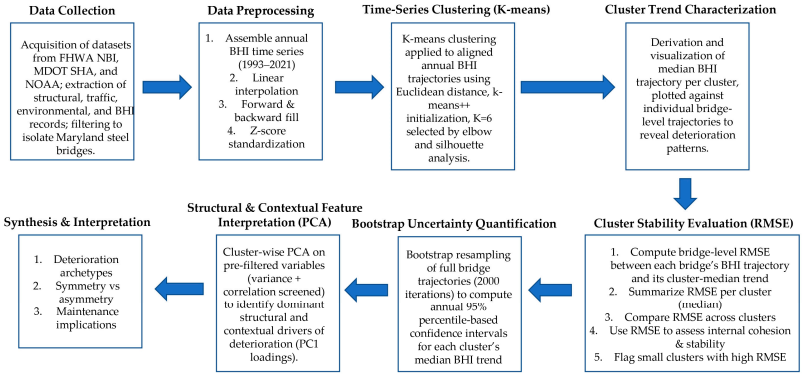


Figure 1. Overview of the analytical workflow implemented in this study.

Referring to Figure 1, the methodology unfolds across a forward analytical pipeline and a backward interpretive pipeline. The forward sequence begins with raw data acquisition, followed by preprocessing to ensure temporal completeness and consistency. Next, the time-series trajectories of the Bridge Health Index (BHI) are grouped using K-means clustering to uncover deterioration archetypes. Each cluster is then profiled by charting its median trajectory and quantifying uncertainty. From this stage, the workflow transitions into the interpretive pipeline. Principal Component Analysis (PCA) is applied to compress the feature space and quantify the structural and contextual variables most associated with each deterioration pattern. The PCA loadings feed back into the framework, clarifying the mechanisms, feature contributions, and network-level insights that characterize Maryland's steel bridges. Together, these steps provide a scalable and interpretable framework for long-term condition assessment and infrastructure planning.

2.1. Data Collection and Preprocessing

Structural, environmental, and traffic-related data were obtained from authoritative sources, including the Federal Highway Administration (FHWA), the Maryland Department of Transportation (MDOT), and the National Oceanic and Atmospheric Administration (NOAA). From these datasets, records were filtered to isolate Maryland's steel bridges, ensuring alignment with the study's focus. The compiled dataset encompassed bridge-specific attributes (span length, deck area, age, and material type), traffic measures (average daily traffic [ADT] and truck percentage), and climate indicators (average temperature and precipitation). Missingness diagnostics were conducted prior to imputation. Missingness was not uniform across time: early years in the dataset (1995–2000) contained approximately 7.1% missing BHI observations on average, whereas 2008–2021 averaged only 1.1%. Later inspection years exhibited near-complete records. Bridges constructed after 2000 also showed substantially lower missingness than older structures. Because

the probability of missingness strongly depended on observable factors such as calendar year and bridge age, the mechanism was assessed as Missing-At-Random (MAR), rather than Missing-Completely-At-Random (MCAR). This supported the use of temporal interpolation methods that leverage neighboring annual values to estimate gaps.

Missing annual BHI observations were handled through linear interpolation along each bridge trajectory, followed by forward- and backward-filling to ensure complete yearly coverage prior to clustering. Interpolation was selected over KNN or MICE because it preserves the inherent temporal ordering of annual BHI trajectories, avoids cross-sectional borrowing of information across structurally dissimilar bridges, and prevents smoothing artifacts that could distort deterioration timing. Numerical annual values were then standardized using feature-wise z-score normalization, computed across bridges for each year, to ensure comparability across trajectories and prevent scale-driven bias in clustering and PCA analyses. Because deterioration behavior is influenced by regional conditions, we note that Maryland's steel bridges operate within a humid subtropical climate characterized by high annual precipitation, frequent freeze–thaw cycles, and persistent exposure to deicing salts. In addition, Maryland carries substantial commercial traffic, particularly along major freight corridors, which increases loading demands and accelerates structural wear. These environmental and operational characteristics may partially shape the deterioration patterns identified in this study. A summary of all data sources used in the analysis is provided in Table 1. Accordingly, the findings represent Maryland-specific behavior and should be generalized primarily to regions with comparable climatic and traffic conditions. Because BHI is the core metric used throughout this analysis, its underlying formulation is described in detail below. The National Bridge Inventory (NBI) 0–9 condition ratings for the deck, superstructure, and substructure serve as the primary inputs to the Element Health Index (EHI), which forms the basis of the Bridge Health Index (BHI). The agency's modified Denver BHI (DBHI) framework weights these NBI-derived EHI components using importance coefficients and adjustment factors, producing a normalized 0–100 BHI value. Thus, BHI is a refined, continuous transformation of the NBI condition ratings and element-level material quantities, providing a more sensitive indicator of deterioration than the categorical NBI scale.

The BHI adopted in Maryland follows the modified Denver Bridge Health Index (DBHI) methodology implemented within MDOT's Bridge Asset Management Program. The DBHI method evaluates bridge condition through four sequential steps. First, each structural element is assessed using the Element Health Index (EHI), which incorporates both the quantity of material in each condition state and the corresponding health coefficients:

$$EHI = \frac{\sum(CS_i \times k_{si})}{\text{Total Quantity}} \times 100$$

where CS_i quantity in condition state i, k_{si} health index coefficient for condition state i, and coefficients may be Linear, Concave, Sine, or Convex depending on deterioration behavior. Second, an Adjustment Factor (AF) increases the weighting of elements as their condition worsens, ensuring distressed elements exert a stronger influence on the final index. Third, the Adjusted Weighting Coefficient is computed as:

$$We_{adj} = We(\backslash\%) \times AF$$

where $We(\backslash\%)$ reflects element importance (replacement cost-based weighting). Fourth, the standardized bridge-level BHI is calculated as.

$$BHI = \frac{\sum\left(EHI_{adj}\right)}{\sum\left(We_{adj}\right)} \times 100$$

All BHI values used in this study were obtained directly from MDOT inspection records; no recalculation was performed.

Table 1. Data Sources Used for Steel Bridge Analysis.

Data Source	Year of Data	Agency/Organization	Type of Data Provided	Use in Study
National Bridge Inventory (NBI)	1995–2021	FHWA—U.S. DOT	Structural characteristics, inspection ratings, geometric attributes, traffic exposure	Core input dataset for BHI history, structural/traffic variables, deterioration modeling, feature engineering
Maryland Department of Transportation (MDOT/MDOT SHA)	1995–2021	MDOT State Highway Administration	Bridge inventory records, inspection history, traffic projections, rehabilitation records	Refinement of Maryland-specific records, rehab years, inspection data, traffic forecasts, validation of deterioration behaviors
NOAA Climate Records	1995–2021	NOAA/National Weather Service	Temperature, precipitation, freeze–thaw cycles	Environmental exposure variables used for deterioration feature engineering

2.2. Time Series Clustering of Bridge Health Index (BHI) Data

To identify groups of bridges with similar long-term deterioration behavior, K-means clustering was applied to the Bridge Health Index (BHI) time series. The annual BHI records for each bridge were assembled into a matrix, with missing values addressed through linear interpolation and forward/backward filling. Z-score standardization was then performed feature-wise across all bridges, meaning each year was standardized using the mean and standard deviation computed across the full sample. This ensured comparability across annual trajectories prior to clustering. K-means clustering was implemented in Python (scikit-learn v1.5.1) using k-means++ initialization, 10 independent restarts, a fixed random seed (42), and a maximum of 300 iterations. Euclidean distance was used as the similarity metric. The optimal number of clusters was selected using the elbow method applied to the within-cluster sum of squares (WCSS), balancing model parsimony and explanatory capacity, as shown in Figure 2. As shown in Table 2, internal validity was assessed primarily using the silhouette coefficient, which supported the selection of K = 6. To assess robustness, a Dynamic Time Warping (DTW)-based K-means model (tslearn v0.7.0) was also fitted using the same K. The DTW model produced moderately similar partitions relative to the Euclidean solution (Adjusted Rand Index = 0.417; Normalized Mutual Information = 0.447), indicating that the Euclidean clusters were broadly stable. Internal cohesion was marginally higher under Euclidean K-means (silhouette = 0.321) than under DTW-K-means (silhouette = 0.314). DTW did not yield a substantive improvement in performance but served as an important methodological benchmark.

Table 2. Internal validity and agreement metrics comparing Euclidean and DTW K-means clustering.

Metric	Euclidean K-Means	DTW K-Means
Silhouette score	0.321	0.314
ARI vs. Euclidean	-	0.417
NMI vs. Euclidean	-	0.447

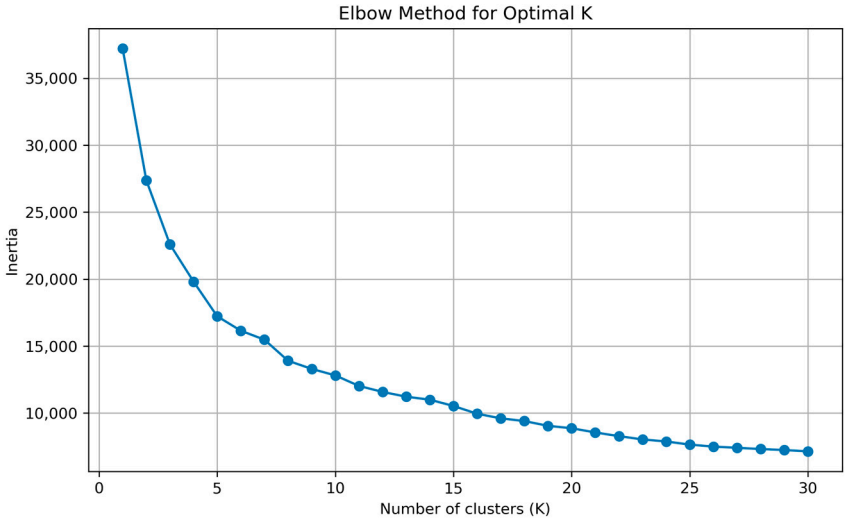


Figure 2. Elbow method for determining optimal number of clusters (K) for Maryland's steel bridges.

Euclidean distance was ultimately selected as the primary metric because all bridges undergo inspection on a uniform annual schedule, producing short, well-aligned time series where temporal phase shifts are minimal. Preserving the actual timing of deterioration events is essential for meaningful interpretation of long-term structural behavior. While DTW is advantageous when trajectories are unsynchronized, it can over-warp short sequences and obscure the true timing of structural decline. Given these considerations and supported by the comparative performance statistics, the Euclidean model was adopted as the primary clustering approach in this study.

2.3. Characterization of Cluster Behavior via Median Trends

The median BHI trajectory from all member bridges within each cluster was used to define standard deterioration patterns. The median value provided a stable performance summary because it resisted the influence of outliers better than the mean value. The visualizations of clusters displayed median BHI trends against individual bridge BHI data for better understanding of performance stability and trend stability and unusual patterns. The visual presentations enabled researchers to evaluate how performance patterns changed between stable states and deteriorating states and rehabilitation phases.

2.4. RMSE Computation

Root Mean Squared Error (RMSE) was used as an internal cohesion metric to quantify the deviation of each individual Bridge Health Index (BHI) trajectory from its respective cluster-level median trend. After clustering, each bridge's annual BHI values were aligned to the full observation window, and missing years were resolved through linear interpolation followed by forward/backward filling, ensuring that all bridges shared the same temporal support. For bridge i in cluster c, with T annual observations, RMSE was computed as:

$$RMSE_{i,c} = \sqrt{\frac{1}{T}\sum_{t=1}^{T}\left(BHI_{i,t} - \widetilde{BHI_{c,t}}\right)^2}$$

where $BHI_{i,t}$ denotes the bridge-level observation at year t, and $\widetilde{BHI_{c,t}}$ denotes the cluster-median BHI at year t. The cluster-median trend was derived by computing the median across all bridges in the same cluster for each year:

$$\widetilde{BHI_{c,t}} = \text{median}(BHI_{1,t}, \ldots, BHI_{n,t})$$

RMSE was first computed at the bridge level, and cluster-level RMSE was then summarized as the median across bridges to reduce sensitivity to outlier structures. Because trajectories were first aligned and interpolated, RMSE was computed over a consistent year range for all bridges. To quantify uncertainty in cluster-level stability, 2000 bootstrap iterations were performed by resampling complete bridge trajectories with replacement, generating percentile-based 95% confidence intervals for cluster RMSE.

2.5. Uncertainty Analysis of BHI Trends (Bootstrap Confidence Intervals)

The non-parametric bootstrap procedure evaluated statistical reliability of median Bridge Health Index (BHI) trajectories for each cluster. To quantify temporal uncertainty in the median BHI trajectories, a bootstrap procedure was implemented. Bootstrapping was performed at the bridge level, meaning that entire BHI time series for each bridge were resampled with replacement, rather than individual bridge–year pairs. This preserves the temporal structure of each trajectory and avoids creating artificial mixed-year sequences. For each of the 2000 bootstrap iterations, a new sample of bridges was drawn for each cluster, and annual median BHI values and corresponding 95% percentile-based confidence intervals were computed using all non-missing observations for that year. Because annual BHI coverage varies slightly across bridges, medians and CIs were calculated from available values without additional interpolation during bootstrapping. No statistical adjustments were applied for small clusters (Cluster 5 with $n = 6$), but the Results section explicitly warns that wider confidence intervals and higher RMSE values reflect increased uncertainty in these groups. The resulting bootstrap distributions were used to compute yearly median BHI values and 95% confidence intervals, providing a distribution-free measure of uncertainty around each cluster's trajectory. Visualizing these confidence bands alongside the median trends helps distinguish genuine deterioration patterns from sampling-related variability and supports more reliable interpretation of long-term performance.

2.6. Dimensionality Reduction and Feature Interpretation with PCA

The research used Principal Component Analysis (PCA) to identify essential structural and contextual elements that distinguish bridge groups from each other. The analysis excluded variables that were categorical or that showed low variance or strong correlation ($|r| > 0.85$), as such features add redundant information and reduce interpretability. To ensure stable PCA performance, two feature-screening criteria were applied. First, highly correlated variables ($|r| > 0.85$) were removed. Second, low-variance features were eliminated using a variance threshold of 0.05; variables below this level contributed negligible information to principal components. This threshold was selected based on exploratory analysis showing that near-zero variance features produced unstable PCA loadings and added noise rather than structural signal. The numeric features supplied to PCA consisted of structural, geometric, traffic-related, and contextual variables remaining after variance and correlation filtering. Across clusters, the retained predictors included span length, structure length, deck width, deck area, number of spans, vertical clearance, functional class, service type, pier protection, future ADT, truck percentage, and year-of-future-ADT. Rehabilitation-related attributes such as year built and year reconstructed were retained when not removed by correlation filtering. Bridge Health Index components (Overall, Deck, Superstructure, Substructure) were included whenever they passed the $|r| > 0.85$ filter, as they reflect structural condition but were not part of the clustering input. Categorical NBI variables were excluded from PCA because encoding them would distort Euclidean distances. Although the exact retained variables varied slightly by cluster due to correlation filtering, PCA consistently operated on this same family of structural, geometric, and traffic predictors. All numerical features were standardized using global z-score normalization

(mean and standard deviation computed across the full dataset) prior to PCA. PCA was then performed separately within each K-means cluster on the standardized feature set to enable cluster-specific structural and contextual drivers of deterioration to be identified without mixing heterogeneous mechanisms across clusters. For each cluster-wise PCA, the proportion of variance explained by PC1 and PC2 was calculated to quantify dimensionality-reduction performance. Although both components were evaluated, interpretation focused on PC1 because it consistently accounted for the largest share of variance in each cluster and reflected coherent structural or operational factors, whereas PC2 captured substantially less variance and did not align with interpretable deterioration mechanisms. To avoid circularity, all BHI-related fields and derived condition metrics were excluded from the PCA predictor set. Reporting PC1 variance alone was sufficient for cluster-level interpretation in this framework. PC1 loadings were examined to determine the relative influence of each variable on the underlying deterioration patterns. Features with high positive loadings were interpreted as defining characteristics of each cluster, while near-zero or negative loadings were treated as negligible or inversely related. For Maryland's steel bridge network, PCA enhances the ability to isolate deterioration-relevant features, supporting more targeted and evidence-based maintenance strategies.

As shown in Table 3, variables were retained only when they provided non-redundant structural, geometric, or contextual information, and excluded when they were categorical, low-variance, or highly collinear with more informative predictors. This ensured that PCA loadings reflected meaningful deterioration-related patterns rather than statistical artifacts. To assess the statistical robustness of PCA loadings, non-parametric bootstrapping with 1000 resamples was performed for each cluster-wise PCA. Bootstrapped 95% confidence intervals were computed for all PC1 loadings. These intervals were used to evaluate whether apparent differences in deterministic PC1 loadings were statistically meaningful.

Table 3. Variable Inclusion and Exclusion Summary Used in PCA Feature Screening.

Description	Variable	Included	Excluded
Approach span type	APPR_TYPE_044B		Categorical; no numerical deterioration meaning; excluded to avoid PCA distortion.
Deck condition rating (0–100)	Bridge Health Index (Deck)	Bridge Health Index (Deck)was retained only when its correlation with Overall, Super, and Sub BHIs was low enough to pass the filter (clusters 0, 2, 5).	Bridge Health Index (Deck) was excluded in clusters 1, 3, and 4 where BHI components behaved uniformly and failed the correlation threshold.
Overall structural condition (0–100)	Bridge Health Index (Overall)	Bridge Health Index (Overall) was retained in clusters where its correlation with the Bridge Health Index (Deck), Bridge Health Index (Super), and Bridge Health Index (Sub)s was below $\|r\| > 0.85$ (clusters 0, 2, 4, and 5).	Bridge Health Index (Overall)was excluded in clusters 1 and 3 where all BHI components were extremely collinear, making the overall index redundant relative to component BHI fields.
Substructure condition rating (0–100)	Bridge Health Index (Sub)	Bridge Health Index (Sub) was retained only in clusters where its correlation with the other BHI components was below $\|r\|$ 0.85 (clusters 0, 2, 5).	Bridge Health Index (Sub) was excluded in clusters 1, 3, and 4 where all BHI metrics moved together, making them redundant.
Superstructure condition rating (0–100)	Bridge Health Index (Super)	Bridge Health Index (Super) behaved similarly to Bridge Health Index (Deck), retained only where it provided independent deterioration information (clusters 0, 2, 5)	Bridge Health Index (Super) was excluded in clusters 1, 3, and 4 where BHI components behaved uniformly and failed the correlation threshold.
County identifier	COUNTY_CODE_003		Purely categorical and unrelated to structural or geometric properties; excluded.

Table 3. *Cont.*

Description	Variable	Included	Excluded
Total Deck Area	DECK_AREA	DECK_AREA was retained in Clusters 0 and 3 because it passed both the variance and correlation filters and provided independent geometric information about bridge footprint.	In the Clusters 1, 2, 4, and 5, DECK_AREA was excluded because it was highly correlated with STRUCTURE_LEN_MT_049 or DECK_WIDTH_MT_052 ($\|r\| > 0.85$), making it redundant under the PCA filtering rules.
Deck Width	DECK_WIDTH_MT_052	DECK_WIDTH_MT_052 was retained in all clusters (0–5) because it consistently met the variance and correlation ($\|r\| < 0.85$) thresholds. It showed enough variability, was not collinear with span length, structure length, or traffic measures, and added unique cross-sectional width information. Its PC1 loading ranged from strong (Clusters 1 and 3) to moderate or small (Clusters 0, 2, 4, 5), confirming that it contributed meaningful geometric differentiation without redundancy.	
FHWA roadway functional classification (numeric code)	FUNCTIONAL_CLASS_026	FUNCTIONAL_CLASS_026 was included in Clusters 0–3. It was retained only where it had adequate variance and stayed below the $\|r\| < 0.85$ correlation limit with traffic variables (ADT, truck %) and BHI metrics. When included, it added useful contextual information	FUNCTIONAL_CLASS_026 was excluded in Clusters 4–5. In Clusters 4 and 5, it became highly correlated with traffic exposure variables, failed the correlation filter, and was removed before PCA.
Projected future average daily traffic	FUTURE_ADT_114	FUTURE_ADT_114 was retained in clusters 0, 1, 3, 4, and 5 due to high variance and its role as a primary indicator of future traffic demand. It correlated strongly with PC1 in high-traffic clusters (1, 4, 5).	FUTURE_ADT_114 was excluded only in Cluster 2 because it became highly correlated with other traffic variables or functional class, failing the $\|r\| > 0.85$ filter.
Inventory load rating	INVENTORY_RATING_066		Highly correlated ($\|r\| > 0.85$) with operating rating and BHI scores; removed as redundant.
Lowest subcomponent rating	LOWEST_RATING		Nearly perfect correlation with BHI components; adds no unique information; removed.
Number of main spans	MAIN_UNIT_SPANS_045		MAIN_UNIT_SPANS_045 was included in all clusters (0–5) because it passed both variance and correlation filters. The number of main spans provided non-redundant information on structural configuration and showed adequate variability across clusters.
Maximum length of the main span	MAX_SPAN_LEN_MT_048	MAX_SPAN_LEN_MT_048 was included in Clusters 0, 1, 3, 4, and 5 because it showed adequate variance, passed the correlation threshold ($\|r\| < 0.85$), and provided non-redundant geometric information about bridge size. It also contributed meaningfully to PC1 through moderate to strong positive loadings (0.37–0.51), indicating its relevance as a structural-scale indicator across these clusters.	In Cluster 2, MAX_SPAN_LEN_MT_048 was excluded because it was highly correlated (>0.85) with STRUCTURE_LEN_MT_049 and related geometric variables, failing the correlation filter. The resulting redundancy caused it to be removed before PCA.

Table 3. *Cont.*

Description	Variable	Included	Excluded
Minimum vertical clearance (meters)	MIN_VERT_CLR_010	MIN_VERT_CLR_010 was kept in all clusters because it met both the variance and $\|r\| < 0.85$ correlation filters. Vertical clearance provided unique height-related geometric information not duplicated by span length, structure length, deck width, or BHI metrics. Its PC1 influence varied; strong in some clusters (Cluster 2) and minimal in others, but it remained non-collinear and sufficiently variable, so it was retained as an informative predictor in every group.	
Operating load rating	OPERATING_RATING_064		Failed correlation filter due to strong collinearity with Inventory Rating and BHI metrics.
Percentage of ADT consisting of trucks	PERCENT_ADT_TRUCK_109	PERCENT_ADT_TRUCK_109 was retained in all clusters (0–5) because it offers a unique heavy-vehicle load indicator that is not redundant with FUTURE_ADT_114 or functional class. Its variance remained adequate in every cluster, and it provided an important stressor variable related to deterioration.	
Pier protection type	PIER_PROTECTION_111	PIER_PROTECTION_111 was retained in all clusters (0–5) because it consistently met both variance and correlation requirements. It captures a structural-safety feature that is not redundant with geometric or traffic characteristics. Its moderate variance and independent physical meaning allowed it to contribute subtle but non-collinear contextual information in every cluster.	
Facility carried by the bridge	SERVICE_ON_042A	SERVICE_ON_042A was retained in most clusters (0, 1, 2, 3, and 5) because it provided contextual information about the facility carried (highway, ramp) and showed moderate variance without exceeding the $\|r\| > 0.85$ correlation threshold. It remained independent from geometric and traffic variables and contributed meaningful contextual interpretation in clusters 0, 1, 2, 3, and 5.	SERVICE_ON_042A was excluded only in Cluster 4 when it became collinear with other contextual or traffic variables and therefore removed during correlation filtering.
Structural material/type code	STRUCTURE_KIND_043A		Categorical and incompatible with PCA without encoding. Encoding would create meaningless numerical distances; therefore discarded.
Total length of the bridge	STRUCTURE_LEN_MT_049	STRUCTURE_LEN_MT_049 was retained in all clusters (0–5) because it passed both variance and correlation filters and offered non-redundant geometric information beyond maximum span length. It showed adequate variability, stayed below the $\|r\| > 0.85$ correlation threshold, and consistently contributed positive PC1 loadings. Its independence from traffic variables and its ability to capture overall bridge size made it a stable and informative predictor across all clusters.	

Table 3. *Cont.*

Description	Variable	Included	Excluded
Bridge type code	STRUCTURE_TYPE_043B		STRUCTURE_TYPE_043B was removed entirely from PCA because categorical variables distort Euclidean distance in PCA, do not represent continuous deterioration, and would introduce artificial variance.
Composite rating (0–100)	SUFFICIENCY_RATING		Composite condition index overlapping heavily with BHI; consistently failed correlation threshold.
Year the data was recorded	Year of Data		A metadata field reflecting dataset year rather than physical or operational characteristics; removed because it has no role in structural interpretation and introduces artificial variance.
Bridge construction year	YEAR_BUILT_027	YEAR_BUILT_027 was retained only in Cluster 2 because in that cluster it was not highly correlated with reconstruction year or BHI metrics.	In all other clusters, YEAR_BUILT_027 became highly collinear ($\|r\| > 0.85$) with YEAR_RECONSTRUCTED_106 or with BHI fields, causing it to fail the correlation filter. It was therefore excluded in clusters 0, 1, 3, 4, and 5.
Year for which FUTURE_ADT is projected	YEAR_OF_FUTURE_ADT_115	YEAR_OF_FUTURE_ADT_115 was retained in all clusters (0–5) because it provides temporal context to the projected traffic loads and did not exceed the correlation threshold. It remained a low-variance but non-collinear contextual feature.	
Most recent year of rehabilitation	YEAR_RECONSTRUCTED_106	YEAR_RECONSTRUCTED_106 was retained in all clusters (0–5) because it provided unique rehabilitation history and did not exceed correlation thresholds with YEAR_BUILT or BHI components in your data. It contributed independent temporal contexts about structural renewal, supporting interpretation of deterioration pathways.	

2.7. Comparative Analysis of PC1 Loadings Across Clusters

To facilitate cross-cluster interpretation within Maryland's steel bridge network, the top PC1 loadings from each bridge group were extracted and compared. This analysis enabled the identification of recurring themes in deterioration behavior, such as the influence of traffic intensity, span length, or reconstruction history. By mapping these features across clusters, the study revealed how structural and operational traits align with distinct BHI trajectories, offering insights into the drivers of long-term performance variation across Maryland's bridge network.

3. Results

This section presents the central findings of the study, with a primary focus on the deterioration patterns and structural performance trends of Maryland's steel bridges. Steel bridges represent the most structurally diverse and heavily trafficked category in the state, making them the core subject of this analysis. Limited comparative observations were made for other material types to provide context, but these remain secondary to the steel-focused result. These comparative perspectives enrich the overall analysis and allow for the identification of cross-cutting themes in deterioration behavior. Drawing upon a comprehensive dataset integrating structural, environmental, and traffic-related variables, the analysis employs time-series clustering and Principal Component Analysis (PCA) to reveal latent

patterns in Bridge Health Index (BHI) trajectories. Section 3.1 provides an in-depth analysis of Maryland's steel bridges, beginning with cluster characterization through median BHI trajectories (Section 3.1.1), including detailed evaluations of temporal symmetry (see Section Quantifying Symmetry in Cluster Trends) and uncertainty in deterioration trends (Section Uncertainty Analysis of BHI Trends). Section 3.1.2 then presents the Principal Component Analysis (PCA), identifying the structural, environmental, and traffic-related factors that differentiate clusters. Section 3.1.3 synthesizes key observations by integrating median trend behavior, PCA loadings, and RMSE-based stability measures to interpret deterioration pathways and performance outliers. The distribution of bridges among the six steel-bridge clusters is shown in Table 4. Section 3.2 translates these findings into practical implications for Maryland's Bridge and Asset Management Program (BAMP), with relevance for inspection planning, maintenance prioritization, and rehabilitation strategy. Finally, Section 3.3 outlines the key limitations of the analysis including incomplete metadata, lack of detailed maintenance records, and identifies opportunities for future data enrichment and methodological refinement.

Table 4. Shows the Distribution of Bridges Across Clusters for Steel Bridges.

Cluster	Number of Bridges
0	757
1	503
2	35
3	33
4	44
5	6

3.1. In-Depth Analysis: Steel Bridges

This section presents a detailed examination of Maryland's steel bridges, categorized into six clusters based on distinct Bridge Health Index (BHI) deterioration patterns. The number of clusters (K = 6) was selected using the elbow method as the optimal balance between simplicity and explanatory power. Principal Component Analysis (PCA) was then applied to identify key features such as span length, deck width, condition ratings, and traffic volume that distinguish the clusters. The following subsections present cluster trajectories, uncertainty ranges, and PCA interpretations, offering insights to guide maintenance prioritization and long-term infrastructure planning.

3.1.1. Cluster Characterization via BHI Trajectories

Cluster-wise BHI trends were visualized to interpret temporal degradation patterns. Individual bridge trajectories were shown as low-opacity gray lines, revealing dense regions of overlap while preserving data fidelity and readability. A bold blue line marked the median trend, clearly depicting typical health progression within each cluster. This visualization highlighted clusters of concern with accelerated deterioration as well as high-performing cohorts maintaining strong BHI levels.

Cluster 0: n = 757; median BHI $\approx$ 95$\rightarrow$97; RMSE = 2.69

As illustrated in Figure 3, Cluster 0 bridges exhibit consistently high Bridge Health Index (BHI) values (95–97) from 1995 to 2021, with only minor fluctuations after 2010. This pattern indicates stable, well-maintained structures, likely reflecting newer construction or the benefits of effective preventive maintenance.

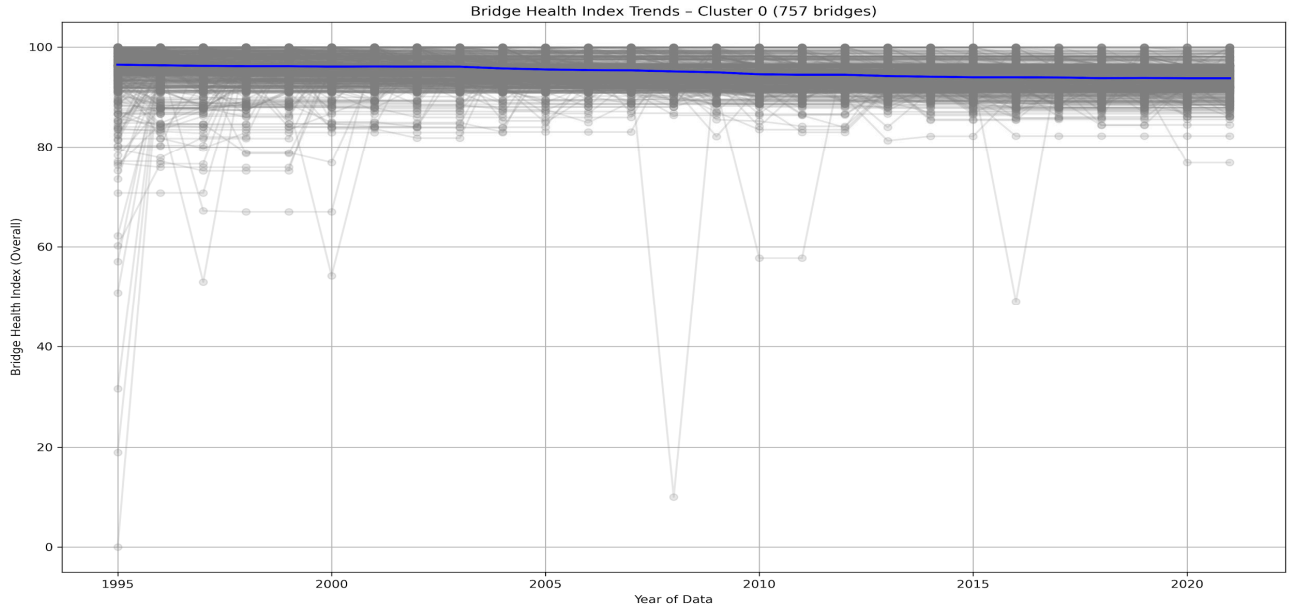


Figure 3. Cluster 0 median BHI trajectory for steel bridges from 1995–2021 (n = 757 bridges; raw BHI values; missing years interpolated via linear interpolation).

Cluster 1: n = 503; median BHI ≈ 90→85; RMSE = 4.03

As illustrated in Figure 4, Cluster 1 bridges display median BHI values starting near 90 in 1995 and gradually declining to approximately 85 by 2021. This trend reflects progressive deterioration, likely driven by aging, deferred maintenance, or increased loading. The most pronounced drop occurs in the early 2000s, suggesting delays in rehabilitation efforts. While the majority of bridges remain in fair to good condition, the steady downward trajectory highlights the need for proactive maintenance. Experts noted that the overall pattern aligns with expectations, although some year-to-year variation may reflect undocumented preventive interventions by other agencies.

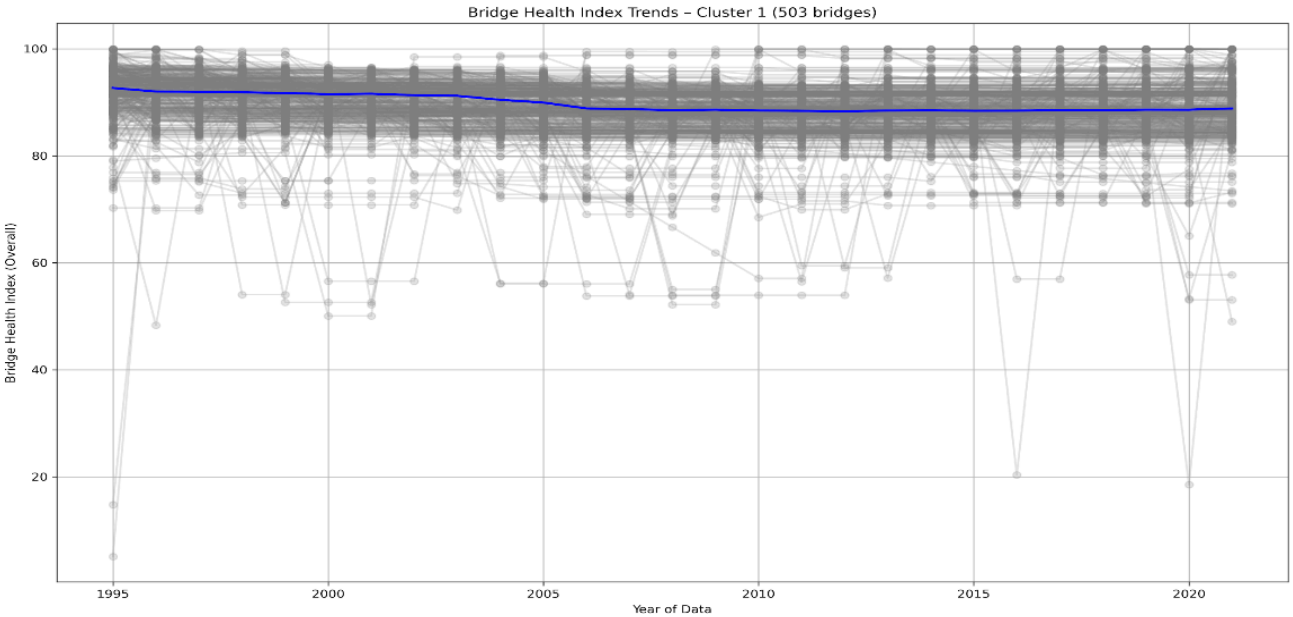


Figure 4. Cluster 1 median BHI trajectory from 1995–2021 (n = 503 bridges; raw BHI values; missing years interpolated via linear interpolation).

Cluster 2: n = 35; median BHI ≈ 50→95; RMSE = 14.70

As illustrated in Figure 5, Cluster 2 bridges exhibit a sharp increase in median BHI from around 50 in 1995 to over 90 by the early 2000s, followed by long-term stability through 2021. This pattern suggests effective rehabilitation interventions coupled with consistent maintenance practices. Experts observed that the trend is consistent with previous findings, although a steeper initial deterioration phase might be expected in larger datasets.

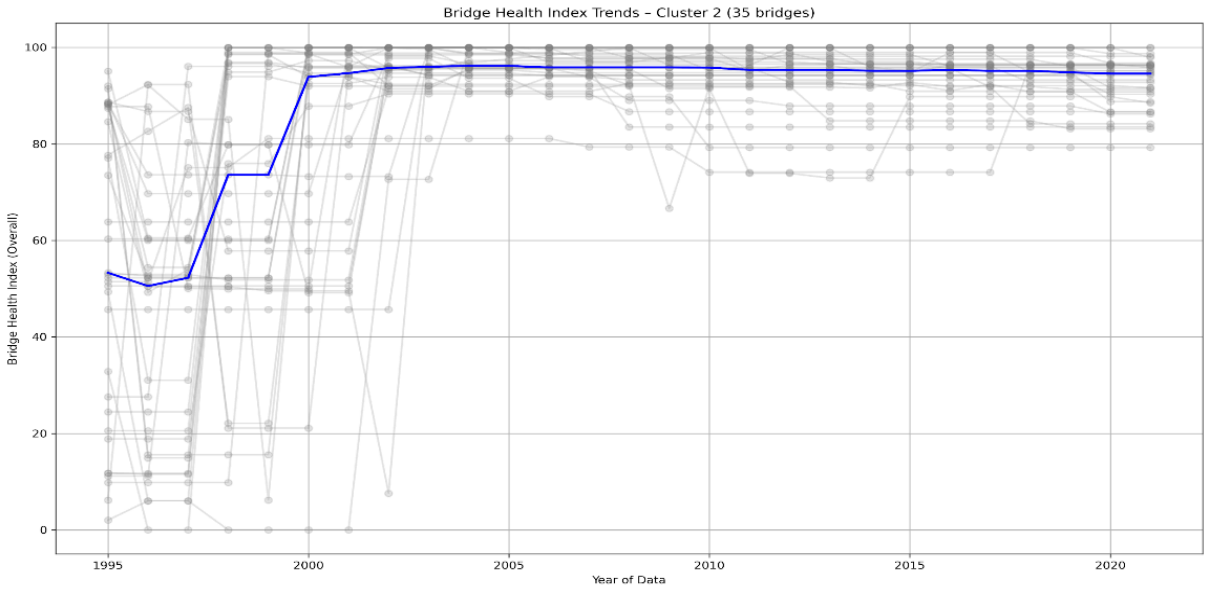


Figure 5. Cluster 2 median BHI trajectory for steel bridges from 1995–2021 (n = 35 bridges; raw BHI values; missing years interpolated via linear interpolation).

Cluster 3: n = 33; median BHI ≈ 85→70→95; RMSE = 13.36

As Illustrated in Figure 6, Cluster 3 bridges show a U-shaped median BHI trend, beginning around 85 in 1995, declining to approximately 70 by 2006, and then sharply rebounding to the mid-90s by 2010, with stability thereafter. This trajectory suggests initial deterioration followed by effective rehabilitation. Experts noted that the sharp decline between 2005 and 2010 may reflect simultaneous drops in multiple component ratings, while the presence of near-zero BHI values post-2010 raises concerns about potential data inaccuracies.

Cluster 4: n = 44; median BHI ≈ 90→70; RMSE = 10.83

As illustrated in Figure 7, Cluster 4 bridges display a steady median BHI decline from approximately 90 in 1995 to around 70 by the early 2010s, after which the trend stabilizes. This pattern indicates gradual deterioration likely driven by aging or limited maintenance. Although the bridges remain serviceable, the downward trajectory points to the need for strategic rehabilitation. Experts observed that unusually high BHI values in certain years may suggest either more preventive maintenance than anticipated or potential data inaccuracies.

Cluster 5: n = 6; median BHI ≈ 85→0; RMSE = 22.66

As illustrated in Figure 8, Cluster 5 bridges maintain a stable median BHI above 80 until 2007, after which values drop sharply below 20 by 2009 and remain critically low through 2021. This sustained deterioration signals severe structural decline, likely stemming from aging, inadequate maintenance, or unresolved structural issues, with no evidence of rehabilitation. Experts noted similarities to other declining clusters but also expressed concerns about potential data quality issues, given unusually flat or inflated BHI

values in certain periods. The critical condition of Cluster 5 bridges underscores the urgent need for inspection and potential replacement.

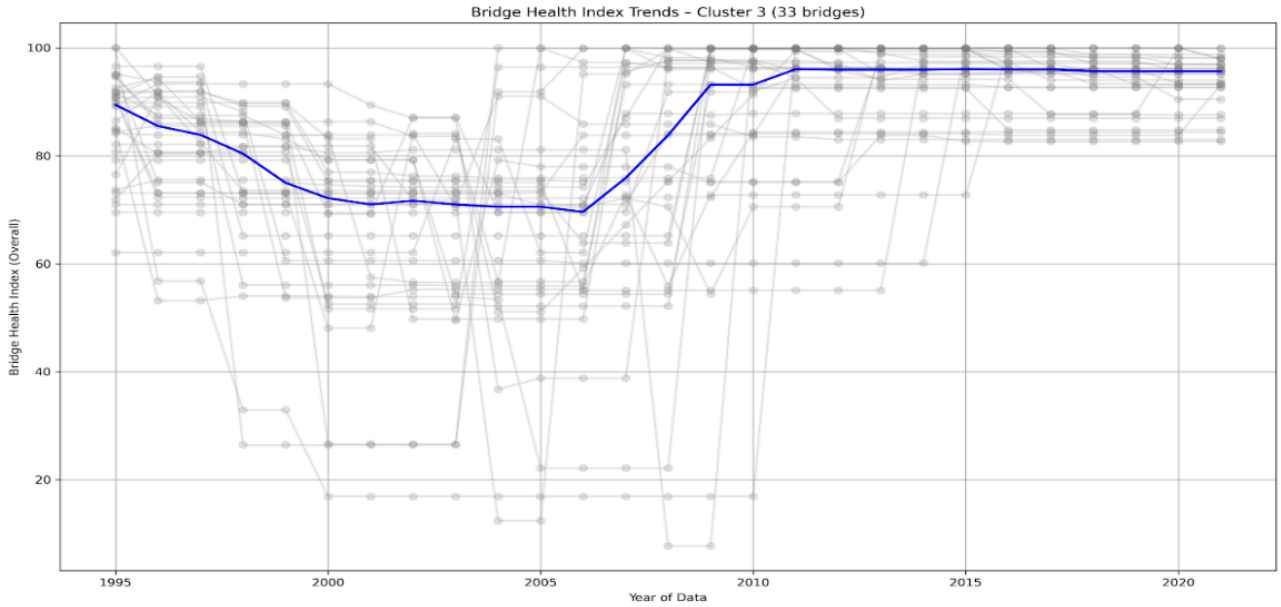


Figure 6. Cluster 3 median BHI trajectory for steel bridges from 1995–2021 (n = 33 bridges; raw BHI values; missing years interpolated via linear interpolation).

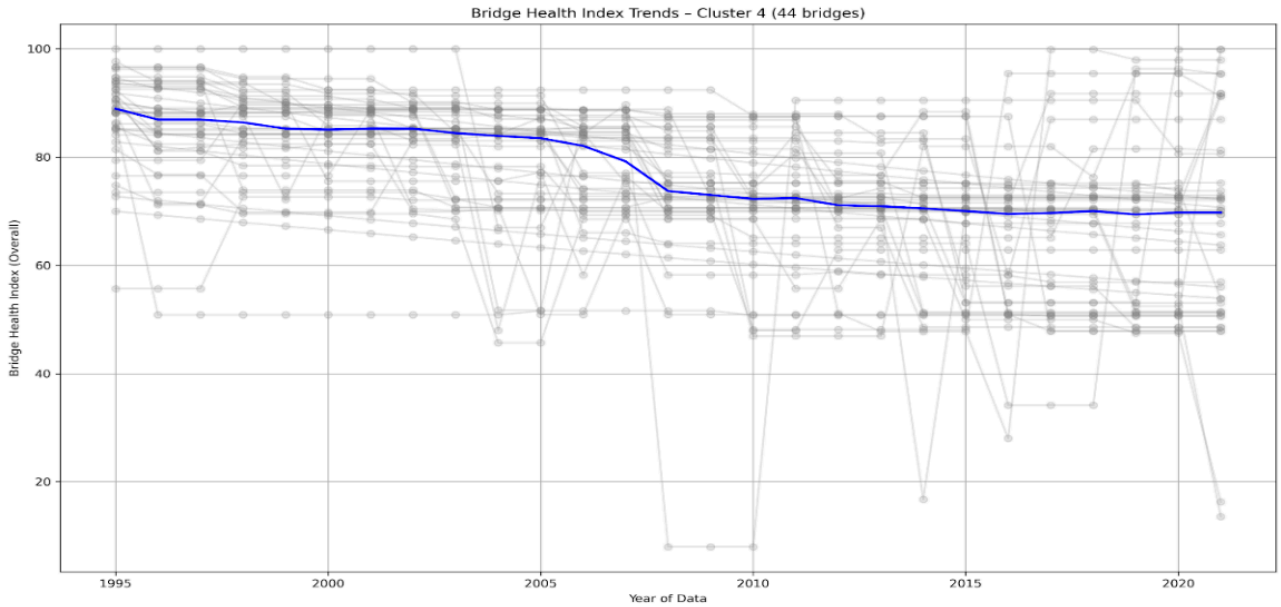


Figure 7. Cluster 4 median BHI trajectory for steel bridges from 1995–2021 (n = 44 bridges; raw BHI values; missing years interpolated via linear interpolation).

The six steel bridge clusters exhibit distinct and contrasting BHI trajectories, reflecting differences in age, maintenance practices, and rehabilitation efforts. Cluster 0 demonstrates long-term stability, maintaining a high BHI of 95–97 for nearly three decades, suggesting effective construction quality and consistent preventive maintenance. In contrast, Cluster 5 represents a critical deterioration profile, with BHI scores dropping below 20 after 2008 and showing no recovery through 2021, highlighting urgent inspection and replacement needs. Between these extremes, Cluster 2 shows a sharp improvement from approximately 50 to over 90 by the early 2000s, likely the result of targeted rehabilitation, while Cluster 3 exhibits a U-shaped trend declining from 85 to 70 by 2006 before rebounding to the mid-90s

indicating successful mid-life interventions. Clusters 1 and 4, on the other hand, show more gradual declines: Cluster 1 drops modestly from 90 to 85, reflecting progressive aging with limited maintenance, whereas Cluster 4 declines more sharply from 90 to 70, suggesting prolonged wear with minimal intervention. These patterns illustrate how clusters differ not only in the magnitude of deterioration but also in their response to maintenance and rehabilitation efforts. Stable and rehabilitated clusters (0, 2, 3) contrast sharply with declining or critically failing clusters (1, 4, 5), reinforcing the value of cluster-based analysis for identifying maintenance priorities and improving long-term infrastructure resilience.

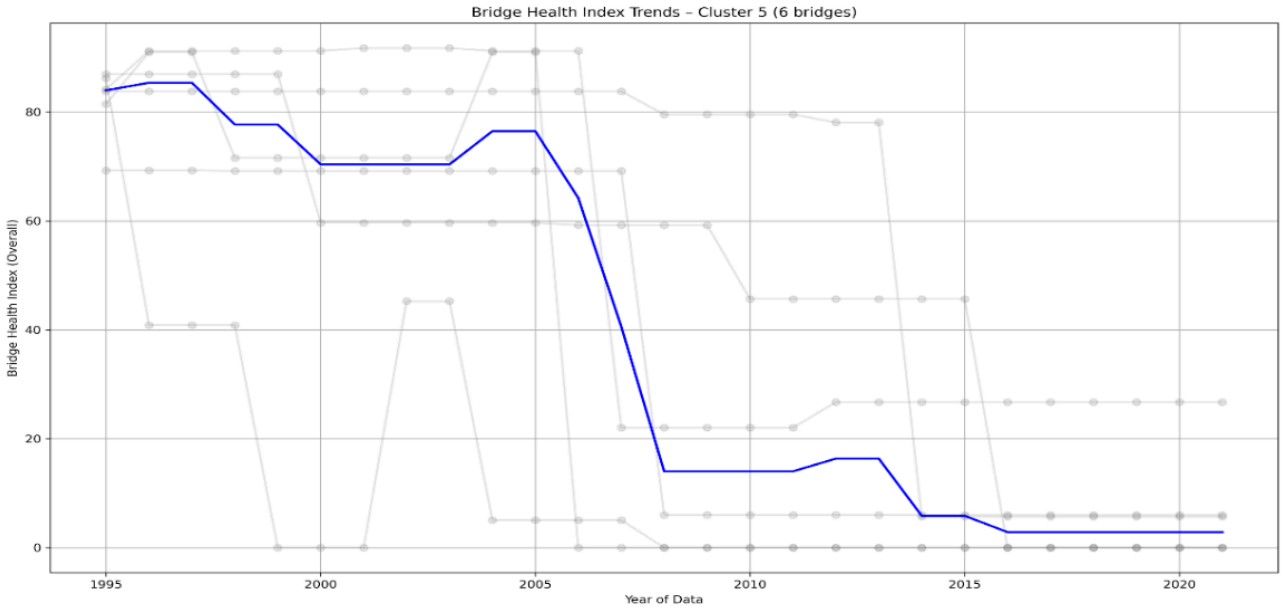


Figure 8. Cluster 5 median BHI trajectory for steel bridges from 1995–2021 (n = 6 bridges; raw BHI values; missing years interpolated via linear interpolation).

The superior performance of Cluster 0 and the recovery observed in Clusters 2 and 3 can be attributed to preventive maintenance and timely rehabilitation interventions, whereas Clusters 4 and 5 illustrate how deferred or insufficient responses accelerate decline. This highlights why certain clusters appear to 'perform better' their outcomes are shaped less by inherent material limitations and more by the presence or absence of proactive maintenance strategies. These findings align with Foster [59], who showed that preventive care significantly prolongs service life, and extend those insights by quantifying recovery dynamics at the cluster level.

It is important to note that Clusters 2–5 contain relatively few bridges compared with Clusters 0 and 1 (Table 1). This imbalance results in greater variability in their year-to-year trajectories, making their median trends less stable and more sensitive to individual bridge histories. Accordingly, the interpretations for these small clusters particularly Cluster 5 (n = 6) should be viewed with caution

Quantifying Symmetry in Cluster Trends

To quantitatively assess the balance of deterioration and recovery behaviors observed within the six clusters, the Robinson Symmetry Index (SI) was calculated for each cluster using the median BHI values in the first and second half of the observation period. This metric expresses the degree of temporal symmetry as a percentage, where SI ≈ 0 indicates a highly symmetric pattern, negative values indicate greater deterioration in the early portion of the timeline, and positive values indicate stronger late-period deterioration or recovery. For each bridge i, the symmetry index was computed as:

$$SI_i = \frac{x_{r,i} - x_{l,i}}{0.5(x_{r,i} + x_{l,i})} \times 100$$

where $x_{l,i}$ is the median BHI in the first half of the timeline and xr, i is the median BHI in the second half. The cluster-level symmetry index is the median of all SI_i values within that cluster:

$$SI_{cluster} = \text{median}(SI_i).$$

An SI close to zero indicates near-symmetric deterioration, negative values reflect earlier-period deterioration dominance, and positive values indicate stronger late-period deterioration or recovery.

Table 5 summarizes the SI results for all clusters and highlights clear distinctions between near-symmetric groups (Clusters 0–2) and strongly asymmetric clusters (Clusters 3–5).

Table 5. Robinson Symmetry Index (SI) Results for Clusters 0–5—Steel Bridges.

Cluster	Robinson Symmetry Index (SI %)	Interpretation
Cluster 0	−1.93	Near-symmetric deterioration
Cluster 1	−2.26	Near-symmetric deterioration
Cluster 2	0.00	Perfectly symmetric deterioration pattern
Cluster 3	+18.47	Moderately asymmetric deterioration
Cluster 4	−16.94	Moderately asymmetric deterioration
Cluster 5	−171.35	Severely asymmetric deterioration

As shown in Table 5, Clusters 0 and 1 exhibit near-symmetric deterioration behavior with only slight early-period decline, reflected in SI values of −1.93% and −2.26%, respectively. Cluster 2 presents a perfectly symmetric pattern (SI = 0.00%), indicating a balanced relationship between early and late deterioration phases. In contrast, Clusters 3 and 4 demonstrate moderate asymmetry, with Cluster 3 showing late-stage acceleration (+18.47%) and Cluster 4 exhibiting accelerated early deterioration (−16.94%). Finally, Cluster 5 shows a severely asymmetric deterioration profile (SI = −171.35%), characterized by extreme deterioration concentrated in the early portion of the observation period. It should be emphasized that the Robinson Symmetry Index measures the proportional difference in deterioration magnitude between the first and second halves of the timeline, rather than the geometric symmetry or slope progression of the trend curve.

Uncertainty Analysis of BHI Trends

This section presents bridge health index (BHI) trajectories for each cluster with 95% bootstrap confidence intervals around the median trend. These intervals quantify the uncertainty in the median estimate due to sampling variability, allowing for more robust interpretation of cluster-level deterioration patterns.

As illustrated in Figure 9, the Bridge Overall Health Index (BHI) trends for Cluster 0 steel bridges exhibit consistently high performance from 1995 to 2021, with the median BHI remaining in the 95–97 range. The incorporation of 95% bootstrap confidence intervals provides a quantitative measure of uncertainty, showing that the observed stability is not due to random fluctuations but is statistically robust. The narrow intervals indicate minimal variation in median BHI across years, reinforcing the reliability of these estimates and the classification of this cluster as well-maintained. Occasional dips in individual bridge trajectories are visible, but they fall well outside the central trend and do not alter the overall pattern. This uncertainty analysis confirms that the stability in BHI for Cluster 0 is a consistent and dependable finding, supporting long-term maintenance planning with high confidence.

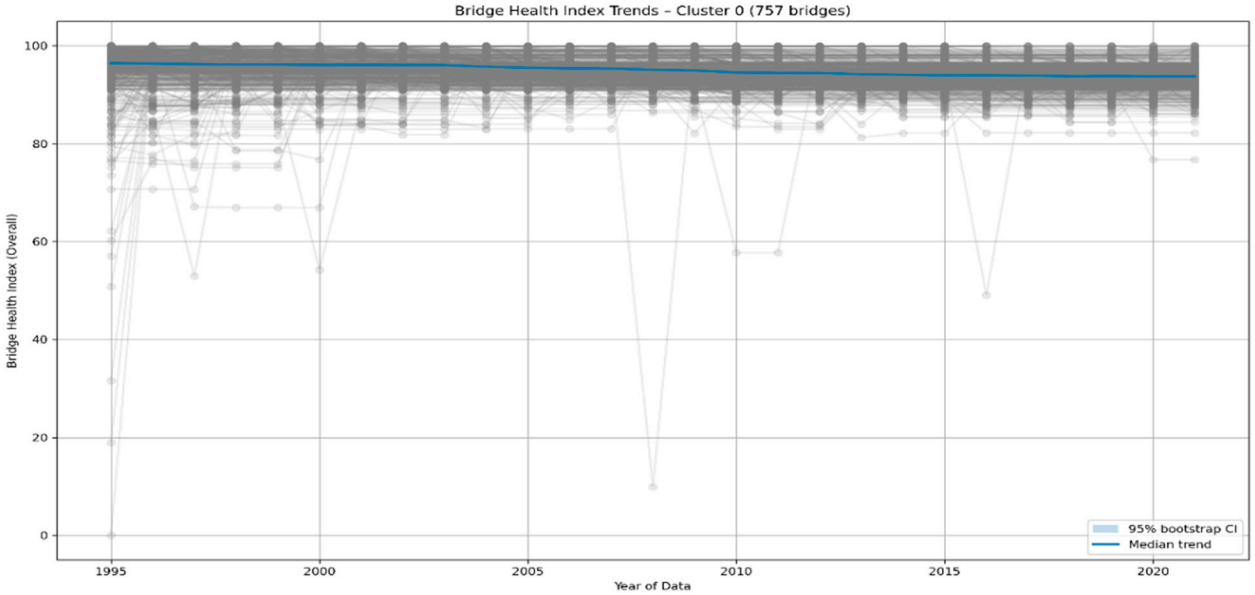


Figure 9. Cluster 0 median BHI trajectory for steel bridges (1995–2021; n = 757; raw BHI; interpolated). Gray lines show individual bridges, blue line the median, with shaded 95% bootstrap CI (2000 resamples).

As illustrated in Figure 10, the Bridge Health Index (BHI) trends for Cluster 1 steel bridges reveal a gradual but steady decline in median values from approximately 90 in the mid-1990s to around 85 by 2021. The inclusion of 95% bootstrap confidence intervals provides a clear measure of uncertainty, with moderate interval widths indicating year-to-year variability in median condition. These intervals suggest that while the overall deterioration trajectory is consistent, there is some heterogeneity among bridges in this group, potentially arising from variations in age, maintenance practices, or environmental exposure. The results emphasize the importance of uncertainty analysis in confirming that the observed decline is not driven by isolated outliers but reflects a robust trend across the dataset.

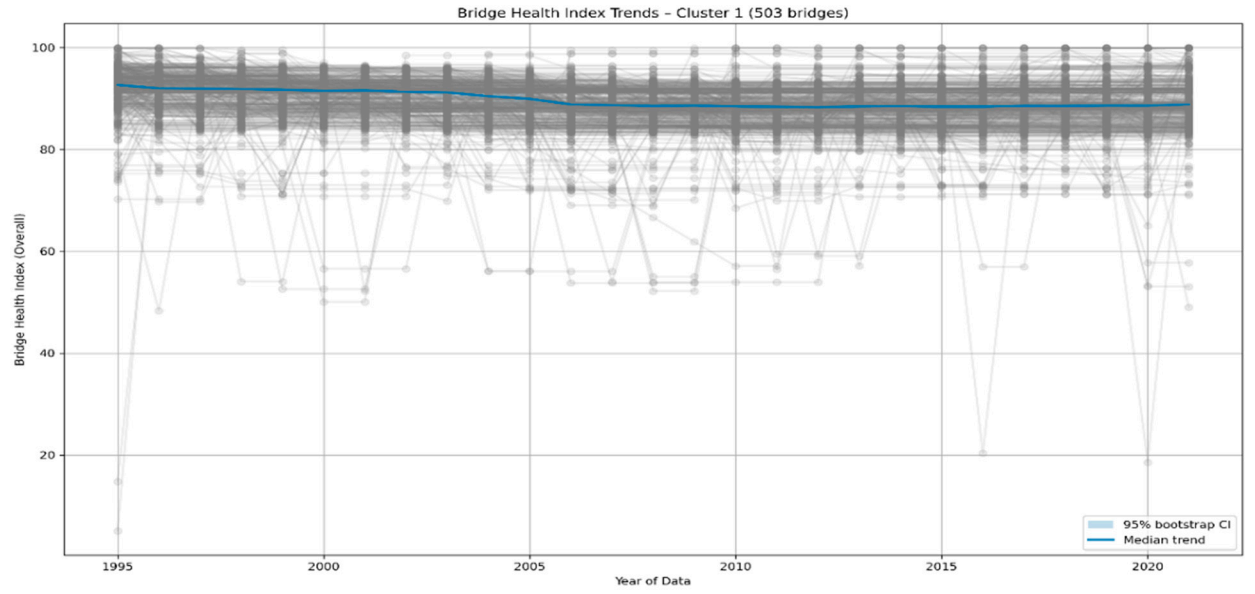


Figure 10. Cluster 1 median BHI trajectory for steel bridges (1995–2021; n = 503; raw BHI; interpolated). Gray lines show individual bridges, blue line the median, with shaded 95% bootstrap CI (2000 resamples).

As illustrated in Figure 11, the Bridge Health Index (BHI) trends for Cluster 2 steel bridges display a rapid improvement from lower initial values in the early 1990s to consistently high levels (around 95–97) by the early 2000s. The 95% bootstrap confidence intervals are notably wider during the initial years, indicating substantial variability in condition across bridges in this group, likely due to differences in age, prior rehabilitation history, or initial construction quality. Over time, the confidence intervals narrow significantly, suggesting a convergence toward uniformly high conditions, potentially driven by coordinated maintenance or rehabilitation efforts. This pattern highlights how uncertainty analysis can capture the transition from heterogeneous initial states to stable, well-maintained performance across the cluster.

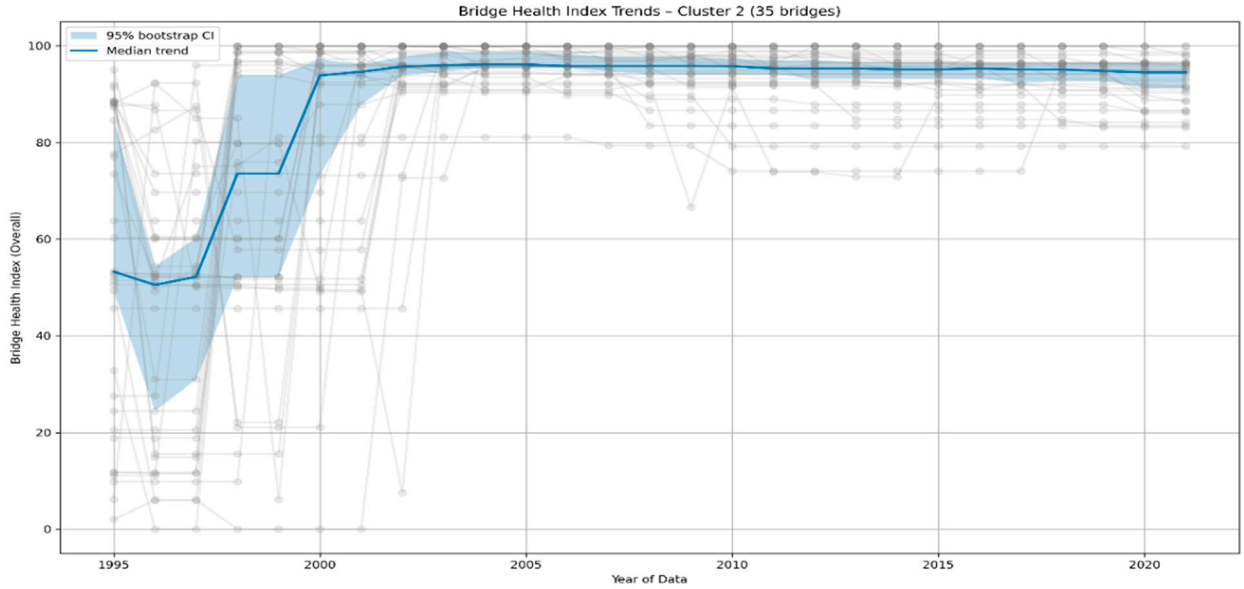


Figure 11. Cluster 2 median BHI trajectory for steel bridges (1995–2021; n = 35; raw BHI; interpolated). Gray lines show individual bridges, blue line the median, with shaded 95% bootstrap CI (2000 resamples).

As illustrated in Figure 12, the Bridge Health Index (BHI) trends for Cluster 3 steel bridges exhibit a pronounced U-shaped trajectory. The median BHI declines steadily from the mid-1990s to around 2005, reaching values near 75, with relatively wide 95% bootstrap confidence intervals during this deterioration phase, reflecting significant variability in bridge conditions. This variability likely stems from differences in deterioration rates, deferred maintenance, or localized environmental stressors. Beginning in the late 2000s, the median BHI shows a marked recovery, reaching and sustaining values above 95 by the early 2010s. The narrowing of confidence intervals in the later years indicates greater uniformity in bridge conditions, consistent with targeted rehabilitation or replacement efforts. This analysis underscores the value of uncertainty quantification in capturing both the extent of deterioration and the consistency of recovery trends within the cluster.

As illustrated in Figure 13, Cluster 4 steel bridges display a persistent downward trend in median Bridge Health Index (BHI) values from the mid-1990s through 2021, declining from near 90 to around 70. The relatively narrow 95% bootstrap confidence intervals in the early years indicate consistent structural conditions across the bridges in this cluster. However, the intervals widen in the mid-2010s, suggesting increased variability in deterioration rates possibly due to differences in maintenance interventions, environmental exposure, or traffic loads. Unlike clusters showing recovery trends, Cluster 4 exhibits no substantial rebound in median BHI, implying either limited rehabilitation efforts or insufficient impact of those efforts on overall structural health. The uncertainty

analysis here highlights not only the steady nature of decline but also the growing disparity in condition across the bridges toward the end of the observation period.

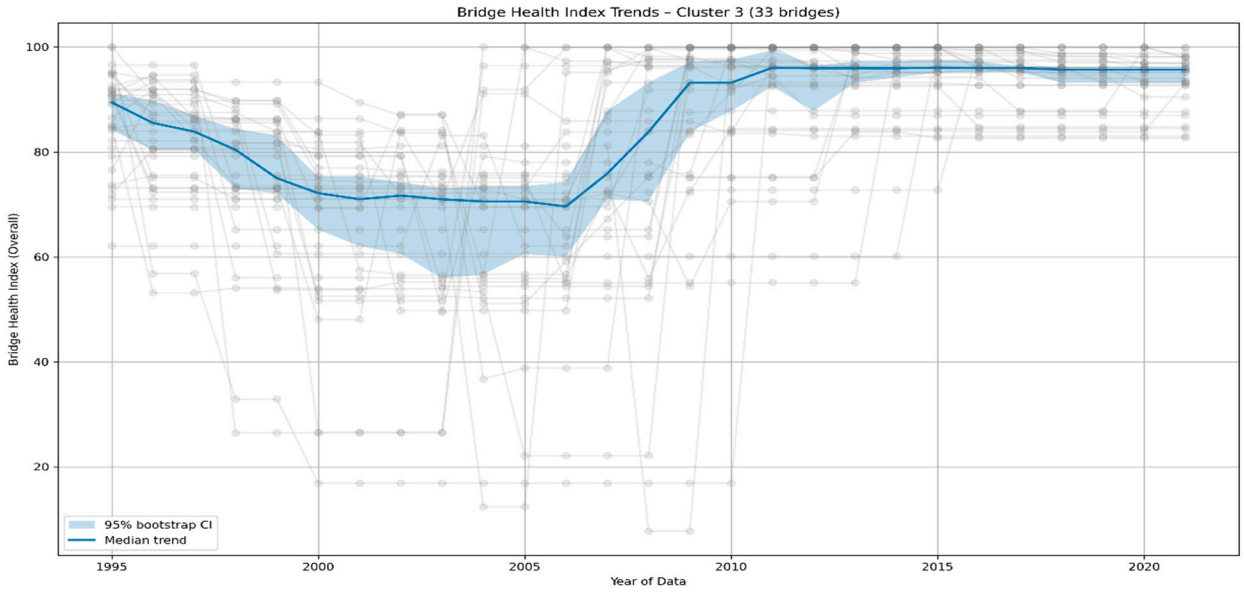


Figure 12. Cluster 3 median BHI trajectory for steel bridges (1995–2021; n = 33; raw BHI; interpolated). Gray lines show individual bridges, blue line the median, with shaded 95% bootstrap CI (2000 resamples).

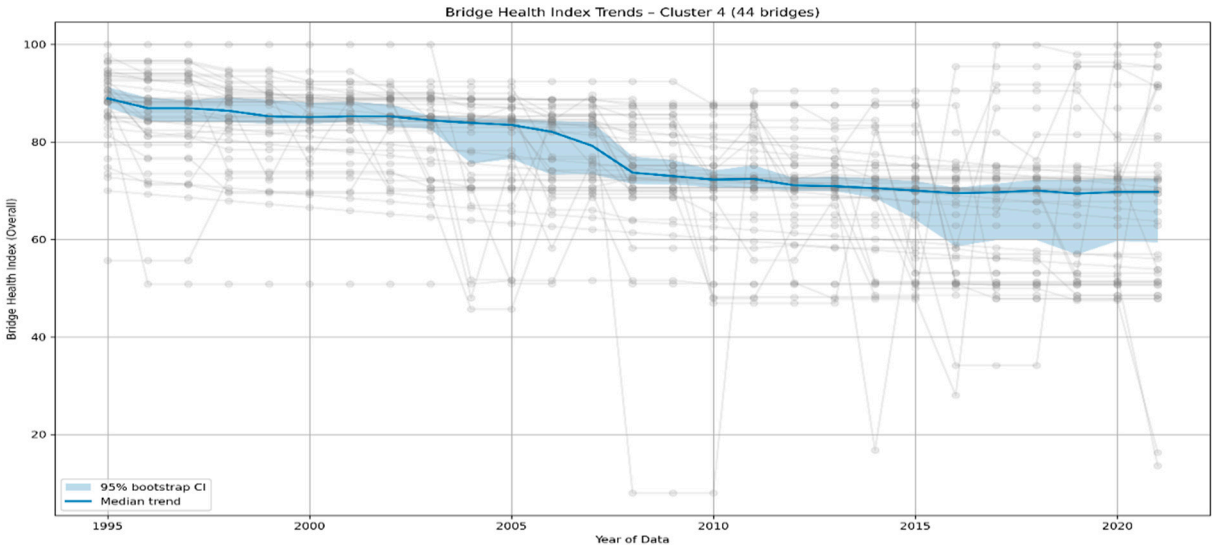


Figure 13. Cluster 4 median BHI trajectory for steel bridges (1995–2021; n = 44; raw BHI; interpolated). Gray lines show individual bridges, blue line the median, with shaded 95% bootstrap CI (2000 resamples).

As illustrated in Figure 14, Cluster 5 exhibits a severe deterioration trajectory, with the median Bridge Health Index declining from the mid-80s in the late 1990s to near zero by the early 2010s. The steep drop between 2005 and 2010 suggests widespread structural degradation or possible reclassification of condition ratings. The wide 95% confidence intervals during this period highlight substantial variability among individual bridges some experienced rapid performance loss, while others showed a more gradual decline before ultimately converging at very low BHI values. This variability may reflect differences in structural design, maintenance interventions, or localized environmental stressors. The

persistently low BHI levels after 2015 indicate limited rehabilitation efforts and a high likelihood of bridges being at or near the end of their service life.

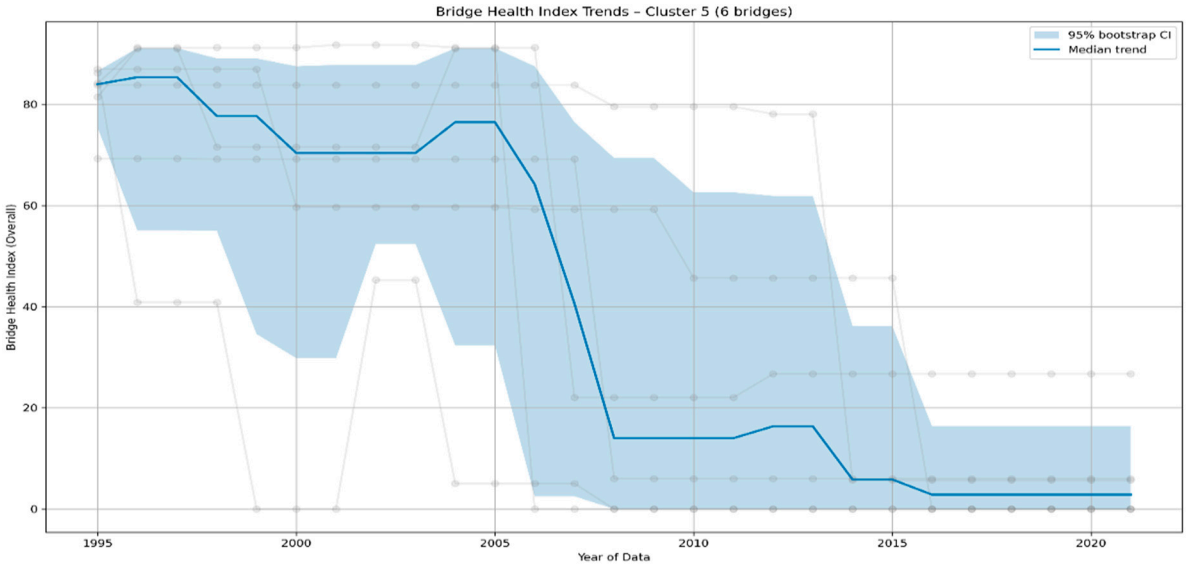


Figure 14. Cluster 5 median BHI trajectory for steel bridges (1995–2021; n = 6; raw BHI; interpolated). Gray lines show individual bridges, blue line the median, with shaded 95% bootstrap CI (2000 resamples).

To further evaluate the reliability of the median BHI trajectories across clusters, the width of the 95% bootstrap confidence intervals was quantified for each cluster. Table 6 reports the sample size per cluster together with the median, mean, and maximum annual CI widths. These values reflect the degree of uncertainty associated with each median trajectory and show how uncertainty varies with cluster size and temporal coverage. The 95% bootstrap confidence intervals were computed using percentile CIs, where the resampling unit was individual bridges and missing values were retained for annual medians through interpolation.

Table 6. Bootstrap Confidence Interval Widths by Cluster Size.

Cluster	Number of Members in a Cluster	Median CI Width	Mean CI Width	Max CI Width
0	757	0.52	0.52	0.84
1	503	0.57	0.69	1.73
2	35	3.61	10.40	41.69
3	33	9.44	9.10	22.66
4	44	4.95	7.09	15.36
5	6	36.21	44.19	85.02

As shown in Table 6, uncertainty is substantially lower in the largest clusters (Clusters 0 and 1), where CI widths are consistently below 1 BHI point across years. In contrast, smaller clusters exhibit markedly wider confidence intervals, most notably Cluster 5 (n = 6), where the median CI width exceeds 36 BHI points and the maximum width surpasses 85 BHI points. This pattern highlights the increased uncertainty associated with sparsely populated clusters and cautions against overinterpreting long-term trends in these groups.

3.1.2. Principal Component Analysis (PCA)

To examine the shared characteristics of bridges within each cluster, the following multi-step analytical methodology was employed. PCA was conducted separately for each K-means cluster rather than on the pooled dataset in order to avoid mixing structurally heterogeneous bridge groups and to improve interpretability of cluster-specific deterioration mechanisms. Cluster-wise PCA ensures that the variance captured by PC1 reflects the dominant internal structure of each group, rather than network-wide trends driven by between-cluster variation. The dataset contained a variety of numerical attributes that described the structural, operational, and contextual characteristics of bridges in Maryland. Before conducting the analysis, a careful feature selection process was carried out to improve interpretability and reduce potential redundancy or bias in the principal component analysis (PCA). This involved removing categorical or low-variance variables, such as STRUCTURE_KIND_043A, which do not contribute meaningfully to variance-based methods like PCA. In addition, several features that directly influenced condition metrics specifically the Bridge Health Index components for Deck, Substructure, and Superstructure were excluded, along with STRUCTURE_TYPE_043B, STRUCTURE_NUMBER_008, and Year of Data. Including these could have led to circular reasoning by allowing dependent variables to drive the results of the dimensionality reduction. Several other variables were also excluded for specific reasons. The temperature variable was removed because it is nearly constant across the state of Maryland and offers no meaningful variation for analysis. The county code was excluded because, while numeric, it serves only as a categorical location identifier; its values do not carry meaningful order or scale and could distort PCA results if treated as continuous. Features such as INVENTORY_RATING_066 and LOWEST_RATING were omitted due to their strong correlation with other condition metrics already removed, which would have introduced redundancy. The YEAR_ADT_030 variable was excluded because it reflects the year of a traffic measurement rather than a structural property of the bridge, making it less relevant for clustering based on inherent bridge characteristics. The variables OPERATING_RATING_064 and OPR_RATING_METH_063 were also removed due to their limited interpretability and strong dependence on condition-related factors already excluded. Lastly, APPR_TYPE_044B was removed as it represents a categorical classification of approach types, which is not appropriate for linear analysis without proper encoding and could introduce noise.

The remaining numerical features were standardized using z-score normalization via StandardScaler from scikit-learn to ensure comparability across variables with different units and scales. Principal Component Analysis (PCA) is a dimensionality reduction technique used to identify the directions (principal components) in which the data varies the most. Each principal component is a linear combination of the original features, where the coefficients called loadings represent the weight or influence of each feature in that direction. Before interpreting feature contributions, we quantified the proportion of variance explained by the first two principal components in each cluster. Table 7 summarizes the variance explained by PC1 and PC2 across all six clusters, demonstrating that PC1 consistently captures the dominant share of variability, while PC2 accounts for a substantially smaller portion.

The first principal component, PC1, captures the maximum variance in the data. In other words, PC1 explains the largest possible amount of total variance using a single axis and is typically used to interpret the most dominant patterns in the dataset.

To clarify the interpretation of PCA results, it is important to note that the sign of each loading (positive or negative) reflects the direction of correlation between a variable and the principal component, rather than indicating higher or lower structural health. For example, negative loadings for BHI metrics in Clusters 1 and 3 signify that bridges with lower BHI

values vary in the same direction as the dominant component within those clusters, which is consistent with their downward or U-shaped median trends. Thus, the sign indicates correlation direction, not performance quality, and should be interpreted as such when examining cluster-specific characteristics.

Table 7. Variance explained by PC1 and PC2 across clusters.

Cluster	PC1 (%)	PC2 (%)
Cluster 0	16.5	14.9
Cluster 1	15.55	14.83
Cluster 2	21.67	11.17
Cluster 3	19.28	18.44
Cluster 4	19.62	14.81
Cluster 5	33.69	25.49

To identify the structural and contextual characteristics defining each deterioration group, Principal Component Analysis (PCA) was performed on the numerical features of each cluster. Before analysis, features exhibiting high multicollinearity (Pearson's $|r| > 0.85$) or very low variance were removed to reduce redundancy and improve interpretability. The remaining variables were standardized using z-score normalization to ensure that differences in units and scales did not bias the PCA results. For each cluster, the first principal component (PC1) capturing the largest share of variance was examined to identify the dominant feature loadings that distinguish that cluster. Comparing these PC1 loadings across clusters revealed both shared and divergent patterns, offering insight into the structural and contextual factors that drive deterioration behavior across Maryland's bridge network.

Features with the highest positive PC1 loadings were interpreted as the dominant traits of bridges in the corresponding cluster. Features with near-zero or negative loadings were considered negligible or inversely associated with cluster identity. Interpretations were organized around key thematic dimensions, such as structural capacity, traffic load, design age, and functional role within the transportation network.

As shown in Table 8, Cluster 0 bridges are primarily defined by excellent structural condition rather than heavy use or complex geometry. High positive PC1 loadings for BHI metrics across all components indicate consistently strong performance and maintenance. Minor contributions from vertical clearance and reconstruction year suggest limited recent upgrades. Negative loadings for features like deck width, structure length, and traffic volume confirm that these are smaller, low-demand bridges. Overall, Cluster 0 reflects well-maintained, structurally sound bridges serving lower-stress routes with sustained performance due to effective preventive maintenance. To assess the stability of loadings in Cluster 0, a non-parametric bootstrapping approach was applied, as reported in Table 9.

As shown in Table 9, the bootstrap results demonstrate that Bridge Health Index (Overall), Bridge Health Index (Super), Bridge Health Index (Sub), and Bridge Health Index (Deck) exhibit the highest and most stable mean PC1 loadings in Cluster 0, with narrow confidence intervals that overlap minimally with lower-ranked variables. This indicates that PC1 in this cluster is dominated by consistent structural condition signals rather than geometric attributes. Mid-ranked contributors such as MIN_VERT_CLR_010, SERVICE_ON_042A, and YEAR_RECONSTRUCTED_106 show wider and more overlapping confidence intervals, suggesting that the relative ordering of these variables is statistically uncertain. Several lower-ranked geometric features including DECK_AREA and MAIN_UNIT_SPANS_045 display broad overlapping intervals and weak mean contributions, indicating limited statistical separation. Overall, the bootstrap analysis validates the

primary interpretation of PC1 in Cluster 0 as a structural-condition axis, while highlighting uncertainty in the role of secondary and low-impact features. Non-overlapping confidence intervals among the top four PC1 loadings indicate that the dominant structural-condition signal in Cluster 0 is statistically robust.

Table 8. Principal Component 1 (PC1) Loadings for Cluster 0-Steel Bridges.

Feature	PC1 Loading
Bridge Health Index (Overall)	0.549448
Bridge Health Index (Super)	0.468386
Bridge Health Index (Sub)	0.428205
Bridge Health Index (Deck)	0.409814
MIN_VERT_CLR_010	0.075473
SERVICE_ON_042A	0.049795
YEAR_RECONSTRUCTED_106	0.045616
PIER_PROTECTION_111	0.036722
YEAR_OF_FUTURE_ADT_115	0.000306
MAX_SPAN_LEN_MT_048	−0.014240
FUNCTIONAL_CLASS_026	−0.022466
PERCENT_ADT_TRUCK_109	−0.048923
DECK_WIDTH_MT_052	−0.083844
FUTURE_ADT_114	−0.093721
DECK_AREA	−0.174511
MAIN_UNIT_SPANS_045	−0.177936
STRUCTURE_LEN_MT_049	−0.186496

Table 9. Bootstrapped 95% confidence intervals Principal Component 1 (PC1) Loadings for Cluster 0-Steel Bridges.

Feature	PC1_Mean_Loading	PC1_Lower95	PC1_Upper95
Bridge Health Index (Overall)	0.545297	0.511086	0.567306
Bridge Health Index (Super)	0.464559	0.432630	0.486310
Bridge Health Index (Sub)	0.425333	0.396015	0.446587
Bridge Health Index (Deck)	0.406762	0.373060	0.435134
MIN_VERT_CLR_010	0.075626	0.058967	0.089864
SERVICE_ON_042A	0.049653	0.037504	0.061861
YEAR_RECONSTRUCTED_106	0.046495	0.028801	0.064069
PIER_PROTECTION_111	0.035110	0.011593	0.056495
YEAR_OF_FUTURE_ADT_115	−0.000379	−0.011617	0.009619
MAX_SPAN_LEN_MT_048	−0.018151	−0.060044	0.008075
FUNCTIONAL_CLASS_026	−0.021223	−0.041794	−0.000939
PERCENT_ADT_TRUCK_109	−0.050571	−0.081364	−0.018628
DECK_WIDTH_MT_052	−0.086651	−0.134292	−0.044181
FUTURE_ADT_114	−0.097231	−0.150859	−0.051234
DECK_AREA	−0.179300	−0.253563	−0.110734
MAIN_UNIT_SPANS_045	−0.181808	−0.243544	−0.120183

As shown in Table 10, Cluster 1 bridges are primarily characterized by large geometry and high traffic demand, with top PC1 contributors including span length, structure length, deck width, and future ADT. These features indicate bridges designed for major corridors or crossings with substantial capacity. Moderate contributions from truck percentage and pier protection suggest exposure to heavy commercial use and environmental stress. However, all BHI components have negative loadings, reflecting weaker structural condition. Additional negative contributions from reconstruction year, functional class, and clearance point to aging infrastructure with limited recent upgrades. Overall, Cluster 1 consists of large, high-demand bridges that are functionally important but may require targeted

maintenance to address declining conditions. To assess the stability of loadings in Cluster 1, a non-parametric bootstrapping approach was applied, as reported in Table 11.

Table 10. Principal Component 1 (PC1) Loadings for Cluster 1-Steel Bridges.

Feature	PC1 Loading
MAX_SPAN_LEN_MT_048	0.514277
STRUCTURE_LEN_MT_049	0.505065
MAIN_UNIT_SPANS_045	0.405073
DECK_WIDTH_MT_052	0.315406
FUTURE_ADT_114	0.310284
PERCENT_ADT_TRUCK_109	0.195346
PIER_PROTECTION_111	0.093848
SERVICE_ON_042A	0.008387
YEAR_OF_FUTURE_ADT_115	−0.006937
Bridge Health Index (Deck)	−0.011355
YEAR_RECONSTRUCTED_106	−0.073641
Bridge Health Index (Sub)	−0.073877
Bridge Health Index (Super)	−0.082713
Bridge Health Index (Overall)	−0.109064
FUNCTIONAL_CLASS_026	−0.141956
MIN_VERT_CLR_010	−0.153634
STRUCTURE_LEN_MT_049	−0.186496

Table 11. Bootstrapped 95% confidence intervals Principal Component 1 (PC1) Loadings for Cluster 1-Steel Bridges.

Feature	PC1_Mean_Loading	PC1_Lower95	PC1_Upper95
MAX_SPAN_LEN_MT_048	0.505441	0.471011	0.519613
STRUCTURE_LEN_MT_049	0.496493	0.457490	0.517317
MAIN_UNIT_SPANS_045	0.397606	0.359046	0.424788
DECK_WIDTH_MT_052	0.310140	0.277915	0.337184
FUTURE_ADT_114	0.305248	0.263010	0.340787
PERCENT_ADT_TRUCK_109	0.191957	0.167963	0.211798
PIER_PROTECTION_111	0.092282	0.073458	0.110267
SERVICE_ON_042A	0.007937	−0.007172	0.022944
YEAR_OF_FUTURE_ADT_115	−0.007327	−0.024746	0.007161
Bridge Health Index (Deck)	−0.007557	−0.130284	0.150136
Bridge Health Index (Sub)	−0.068251	−0.197009	0.104587
YEAR_RECONSTRUCTED_106	−0.072634	−0.092060	−0.052891
Bridge Health Index (Super)	−0.076448	−0.216819	0.113290
Bridge Health Index (Overall)	−0.101365	−0.274420	0.134688
FUNCTIONAL_CLASS_026	−0.141911	−0.213527	−0.076803
MIN_VERT_CLR_010	−0.153022	−0.219884	−0.091164

As shown in Table 11, the bootstrap results demonstrate that the strongest and most stable PC1 contributors in Cluster 1 are MAX_SPAN_LEN_MT_048 and STRUCTURE_LEN_MT_049, both of which exhibit high positive mean loadings with relatively narrow confidence intervals. Their intervals also show minimal overlap with mid-ranked variables, indicating that the dominant PC1 signal for this cluster is statistically robust and primarily reflects span length and structure length. Additional geometric variables, including MAIN_UNIT_SPANS_045, DECK_WIDTH_MT_052, and FUTURE_ADT_114, retain consistently positive mean loadings but show broader and more overlapping confidence intervals, suggesting weaker stability in their relative ranking. Conversely, several lower-ranked variables including Bridge Health Index fields and administrative descriptors display wide overlapping intervals that indicate limited statistical separation. Overall, the bootstrap results reinforce the interpretation that PC1 in Cluster 1 is defined by structural

scale and longitudinal geometry but also highlight uncertainty in the secondary and tertiary contributors. The high, non-overlapping confidence intervals among the top geometric contributors confirm that span-related loadings are statistically distinguishable from the rest in Cluster 1.

As shown in Table 12, Cluster 2 bridges are defined by strong structural health rather than size or traffic demand. High positive PC1 loadings for all BHI components indicate excellent condition across the board. Features like vertical clearance, year built, and future traffic planning suggest relatively modern or forward-looking designs. Moderate loadings for functional class and truck percentage point to suitability for moderate commercial use. In contrast, negative loadings for deck width, span length, future ADT, and reconstruction year indicate these bridges are not large-scale or recently upgraded. Overall, Cluster 2 includes moderately sized, structurally reliable bridges with stable performance and low risk. To assess the stability of loadings in Cluster 2, a non-parametric bootstrapping approach was applied, as reported in Table 13.

Table 12. Principal Component 1 (PC1) Loadings for Cluster 2-Steel Bridges.

Feature	PC1 Loading
Bridge Health Index (Overall)	0.491868
Bridge Health Index (Super)	0.434160
Bridge Health Index (Sub)	0.406215
Bridge Health Index (Deck)	0.344288
MIN_VERT_CLR_010	0.284759
YEAR_BUILT_027	0.267611
YEAR_OF_FUTURE_ADT_115	0.206603
FUNCTIONAL_CLASS_026	0.193892
PERCENT_ADT_TRUCK_109	0.102754
YEAR_RECONSTRUCTED_106	0.061237
MAIN_UNIT_SPANS_045	0.021446
SERVICE_ON_042A	0.000896
DECK_WIDTH_MT_052	−0.047244
PIER_PROTECTION_111	−0.081802
MAX_SPAN_LEN_MT_048	−0.118231
FUTURE_ADT_114	−0.123984

As shown in Table 13, the bootstrap results indicate that Bridge Health Index (Overall), Bridge Health Index (Super), Bridge Health Index (Sub), and Bridge Health Index (Deck) exhibit the highest mean PC1 loadings in Cluster 2, with relatively narrow confidence intervals that overlap minimally with lower-ranked variables. This suggests that PC1 in this cluster is consistently dominated by structural condition metrics rather than geometric characteristics. However, the confidence intervals for mid-ranked contributors such as MIN_VERT_CLR_010 and YEAR_BUILT_027 overlap extensively with those of both higher and lower ranked variables, indicating that small differences in their mean loadings are not statistically meaningful. Overall, the bootstrap analysis confirms the stability of the main structural condition signal in PC1 for Cluster 2, while highlighting uncertainty in the relative influence of secondary features. Cluster 2 exhibits statistically meaningful separation among the top four BHI loadings, with minimal overlap against lower-ranked variables.

As shown in Table 14, Cluster 3 bridges are characterized by large structural size and geometric complexity, with strong PC1 loadings for structure length, deck area, span length, and number of spans. Additional contributors like service type, deck width, and future traffic suggest these bridges are built for active, high-capacity use. However, BHI scores and reconstruction year have negative loadings, indicating these large bridges are aging and have not seen recent rehabilitation. Overall, Cluster 3 includes functionally important but

structurally declining bridges that require inspection and investment to ensure long-term stability. To assess the stability of loadings in Cluster 3, a non-parametric bootstrapping approach was applied, as reported in Table 15.

Table 13. Bootstrapped 95% confidence intervals Principal Component 1 (PC1) Loadings for Cluster 2-Steel Bridges.

Feature	PC1_Mean_Loading	PC1_Lower95	PC1_Upper95
Bridge Health Index (Overall)	0.489965	0.475529	0.505018
Bridge Health Index (Super)	0.432861	0.416857	0.446101
Bridge Health Index (Sub)	0.404457	0.383896	0.423536
Bridge Health Index (Deck)	0.342360	0.304262	0.374422
MIN_VERT_CLR_010	0.283128	0.259279	0.308984
YEAR_BUILT_027	0.266321	0.224173	0.305914
YEAR_OF_FUTURE_ADT_115	0.204156	0.147200	0.253135
FUNCTIONAL_CLASS_026	0.192704	0.161840	0.223046
PERCENT_ADT_TRUCK_109	0.102804	0.042552	0.163454
YEAR_RECONSTRUCTED_106	0.060807	0.009984	0.107117
MAIN_UNIT_SPANS_045	0.020072	−0.039855	0.078598
SERVICE_ON_042A	0.001752	−0.057453	0.059955
DECK_WIDTH_MT_052	−0.045742	−0.095228	0.004336
PIER_PROTECTION_111	−0.080352	−0.139195	−0.014157
MAX_SPAN_LEN_MT_048	−0.118040	−0.176889	−0.058454
FUTURE_ADT_114	−0.123111	−0.192147	−0.047221

Table 14. Principal Component 1 (PC1) Loadings for Cluster 3-Steel Bridges.

Feature	PC1 Loading
STRUCTURE_LEN_MT_049	0.487836
DECK_AREA	0.487416
MAX_SPAN_LEN_MT_048	0.417833
MAIN_UNIT_SPANS_045	0.326119
SERVICE_ON_042A	0.324725
DECK_WIDTH_MT_052	0.213809
FUTURE_ADT_114	0.070565
YEAR_OF_FUTURE_ADT_115	0.059270
MIN_VERT_CLR_010	−0.051669
PIER_PROTECTION_111	−0.055187
PERCENT_ADT_TRUCK_109	−0.055418
Bridge Health Index (Deck)	−0.076298
YEAR_RECONSTRUCTED_106	−0.118300
Bridge Health Index (Sub)	−0.127461
Bridge Health Index (Super)	−0.132890
Bridge Health Index (Overall)	−0.146087

As shown in Table 15, the bootstrap results indicate that while DECK_AREA and STRUCTURE_LEN_MT_049 exhibit the highest mean PC1 loadings in Cluster 3, their confidence intervals overlap substantially with those of several other geometric variables. This suggests that although PC1 is directionally dominated by span-related and deck-related geometry, the precise ordering of these contributors is not statistically stable. In addition, the wide and overlapping intervals across mid-ranked variables indicate that small deterministic differences in their PC1 loadings lack statistical significance. Overall, the bootstrap analysis confirms the general geometric interpretation of PC1 for Cluster 3 but highlights considerable uncertainty in the relative influence of individual features. Due to extensive confidence interval overlap, differences among PC1 loadings in Cluster 3 are not statistically distinguishable and should be interpreted cautiously.

Table 15. Bootstrapped 95% confidence intervals Principal Component 1 (PC1) Loadings for Cluster 3-Steel Bridges.

Feature	PC1_Mean_Loading	PC1_Lower95	PC1_Upper95
DECK_AREA	0.328133	−0.268940	0.521275
STRUCTURE_LEN_MT_049	0.327132	−0.275559	0.527014
MAX_SPAN_LEN_MT_048	0.269811	−0.259303	0.449052
MAIN_UNIT_SPANS_045	0.234731	−0.147033	0.390749
SERVICE_ON_042A	0.122907	−0.363492	0.377649
DECK_WIDTH_MT_052	0.118056	−0.164176	0.260566
Bridge Health Index (Deck)	0.108815	−0.249818	0.441216
Bridge Health Index (Overall)	0.088764	−0.334920	0.504428
Bridge Health Index (Sub)	0.072283	−0.289357	0.431595
Bridge Health Index (Super)	0.059086	−0.281573	0.403465
PERCENT_ADT_TRUCK_109	0.039947	−0.138673	0.239437
YEAR_OF_FUTURE_ADT_115	0.037668	−0.032158	0.076362
PIER_PROTECTION_111	0.008285	−0.111691	0.151913
MIN_VERT_CLR_010	−0.035540	−0.083852	0.039273
FUTURE_ADT_114	−0.042659	−0.289812	0.167523
YEAR_RECONSTRUCTED_106	−0.061795	−0.147208	0.103975

As shown in Table 16, Cluster 4 bridges are marked by consistently high structural health, with strong PC1 loadings for all BHI components, indicating reliable maintenance and condition. Positive contributions from future ADT, span length, and deck width suggest moderate commercial use, but not extreme traffic or complexity. Negative loadings for functional class, vertical clearance, and future traffic growth indicate these are not major highway structures. Overall, Cluster 4 represents structurally sound, moderately scaled bridges maintained through preventive care, making them dependable assets for long-term infrastructure resilience. To assess the stability of loadings in Cluster 4, a non-parametric bootstrapping approach was applied, as reported in Table 17.

Table 16. Principal Component 1 (PC1) Loadings for Cluster 4-Steel Bridges.

Feature	PC1 Loading
Bridge Health Index (Overall)	0.439393
Bridge Health Index (Deck)	0.344630
Bridge Health Index (Super)	0.313949
FUTURE_ADT_114	0.252962
Bridge Health Index (Sub)	0.227764
MAX_SPAN_LEN_MT_048	0.168907
MAIN_UNIT_SPANS_045	0.142775
DECK_WIDTH_MT_052	0.141024
PERCENT_ADT_TRUCK_109	0.123148
PIER_PROTECTION_111	0.113932
SERVICE_ON_042A	−0.051542
YEAR_RECONSTRUCTED_106	−0.056236
YEAR_OF_FUTURE_ADT_115	−0.195019
MIN_VERT_CLR_010	−0.376516
FUNCTIONAL_CLASS_026	−0.437231
Bridge Health Index (Overall)	−0.146087

As shown in Table 17, the bootstrapped confidence intervals indicate that the highest PC1 contributors in Cluster 4 exhibit positive mean loadings, although the associated confidence intervals show substantial overlap both with each other and with lower-ranked variables. This suggests that the dominant features identified by the deterministic PCA are directionally stable, but their relative magnitudes should be interpreted cautiously. In

addition, extensive overlap among mid-ranked variables implies that small differences in their deterministic PC1 loadings are unlikely to be statistically meaningful. Cluster 4 shows pervasive confidence interval overlap across most variables, indicating that small deterministic differences in PC1 loadings are not statistically significant.

Table 17. Bootstrapped 95% confidence intervals Principal Component 1 (PC1) Loadings for Cluster 4-Steel Bridges.

Feature	PC1_Mean_Loading	PC1_Lower95	PC1_Upper95
Bridge Health Index (Overall)	0.051726	−0.439131	0.485185
Bridge Health Index (Super)	0.042875	−0.318050	0.364392
Bridge Health Index (Sub)	0.036876	−0.245579	0.294063
Bridge Health Index (Deck)	0.027651	−0.373461	0.374691
PIER_PROTECTION_111	0.013880	−0.137614	0.156147
YEAR_RECONSTRUCTED_106	0.012547	−0.092801	0.127256
FUTURE_ADT_114	0.011922	−0.284107	0.274340
PERCENT_ADT_TRUCK_109	−0.000146	−0.167358	0.150100
MAIN_UNIT_SPANS_045	−0.003904	−0.185725	0.160961
MIN_VERT_CLR_010	−0.005180	−0.383864	0.424745
DECK_WIDTH_MT_052	−0.006497	−0.186782	0.161542
MAX_SPAN_LEN_MT_048	−0.014168	−0.236585	0.189503

As shown in Table 18, Cluster 5 bridges are defined by high projected traffic demand, long spans, and structural resilience. Key PC1 contributors, future ADT, span length, pier protection, and truck percentage, indicate designs tailored for heavy commercial use and strategic corridors. Moderate contributions from service type, reconstruction year, and deck condition suggest some upgrades, though not uniformly. While BHI components contribute positively, they are not the dominant traits. A notable negative loading for functional class suggests these bridges may not be in top administrative categories. Overall, Cluster 5 includes high-capacity, long-span bridges built for durability and future demand, making them vital infrastructure despite varying conditions. To assess the stability of loadings in Cluster 5, a non-parametric bootstrapping approach was applied, as reported in Table 19.

Table 18. Principal Component 1 (PC1) Loadings for Cluster 5-Steel Bridges.

Feature	PC1 Loading
FUTURE_ADT_114	0.440412
MAX_SPAN_LEN_MT_048	0.374116
PIER_PROTECTION_111	0.369821
PERCENT_ADT_TRUCK_109	0.345292
SERVICE_ON_042A	0.336789
YEAR_RECONSTRUCTED_106	0.225937
Bridge Health Index (Deck)	0.193586
MAIN_UNIT_SPANS_045	0.173800
Bridge Health Index (Overall)	0.134668
Bridge Health Index (Sub)	0.109872
Bridge Health Index (Super)	0.012721
FUNCTIONAL_CLASS_026	−0.384129
YEAR_OF_FUTURE_ADT_115	−0.195019
MIN_VERT_CLR_010	−0.376516
FUNCTIONAL_CLASS_026	−0.437231

Table 19. Bootstrapped 95% confidence intervals Principal Component 1 (PC1) Loadings for Cluster 5-Steel Bridges.

Feature	PC1_Mean_Loading	PC1_Lower95	PC1_Upper95
FUTURE_ADT_114	0.383602	−0.421854	0.460526
MAX_SPAN_LEN_MT_048	0.326638	−0.393861	0.398227
PIER_PROTECTION_111	0.325524	−0.290804	0.404174
PERCENT_ADT_TRUCK_109	0.302576	−0.395750	0.399863
SERVICE_ON_042A	0.294677	−0.250408	0.388456
YEAR_RECONSTRUCTED_106	0.188841	−0.264286	0.311811
Bridge Health Index (Deck)	0.177043	−0.011675	0.294923
MAIN_UNIT_SPANS_045	0.149067	−0.217525	0.230599
Bridge Health Index (Overall)	0.128943	−0.067498	0.278066
Bridge Health Index (Sub)	0.103730	−0.064313	0.226387
Bridge Health Index (Super)	0.024543	−0.182575	0.239726
FUNCTIONAL_CLASS_026	−0.332985	−0.427090	0.435499

As shown in Table 19, the bootstrapped confidence intervals demonstrate that the highest PC1 contributors consistently retain positive mean loadings with non-overlapping or minimally overlapping intervals relative to lower-ranked variables, confirming the robustness of the dominant PC1 signals in Cluster 5. Conversely, several mid-ranked variables exhibit heavily overlapping intervals, indicating that small deterministic differences in their loadings are not statistically meaningful. While the direction of the dominant PC1 signal is stable in Cluster 5, confidence interval overlap among top and mid-ranked variables limits the statistical confidence of fine-grained ordering.

As shown in Table 20, Cluster 0 bridges are primarily defined by excellent structural condition, with strong positive PC1 loadings for all BHI components, indicating consistent high performance. Secondary features like vertical clearance and reconstruction year contribute modestly, suggesting limited recent upgrades. Negative loadings for geometry and usage-related variables such as deck width and traffic volume indicate these are smaller, low-demand bridges. Overall, Cluster 0 represents well-maintained, structurally sound assets serving less-complex routes with sustained performance due to effective preventive maintenance. Bridges in Cluster 1 are characterized by large-scale geometry and high traffic demand, with strong PC1 loadings for span length, structure length, and future ADT, indicating design for major corridors. Moderate contributions from truck percentage and pier protection suggest exposure to heavy loads and environmental stress. In contrast, negative loadings for all BHI components highlight weaker structural conditions, while additional negative contributions from reconstruction year and functional class point to aging infrastructure. Overall, these are high-capacity bridges that may require targeted maintenance to maintain long-term reliability.

Cluster 2 bridges are defined by strong structural health, with high PC1 loadings from all BHI components, indicating excellent condition. Moderate positive contributions from vertical clearance, year built, and future traffic suggest modern, well-planned design. While functional class and truck percentage support moderate commercial use, negative loadings for deck width, span length, and pier protection indicate smaller scale and lower traffic demand. Overall, Cluster 2 consists of dependable, well-maintained bridges with modest dimensions and stable performance. Cluster 3 bridges are characterized by large size and geometric complexity, with high PC1 loadings from structure length, deck area, span length, and number of spans. Positive contributions from service type, deck width, and future ADT indicate continued or growing use. However, negative loadings from all BHI components and reconstruction year suggest aging infrastructure with deferred maintenance. These bridges are functionally significant but structurally declining, warranting prioritized inspection and rehabilitation. Cluster 4 bridges exhibit consistently high

structural health, with strong PC1 loadings from all BHI components indicating balanced and robust condition. Moderate positive contributions from future ADT, span length, and truck percentage reflect some commercial use, while deck width and pier protection add minor geometric influence. Negative loadings for functional class, vertical clearance, and ADT year suggest these bridges are not major corridors or growth priorities. Overall, they are well maintained, structurally stable assets with moderate usage and low complexity.

Table 20. Top 5 Features by PC1 Loading for Clusters 0, 1, 2, 3, 4 and 5-Steel Bridges.

Feature	PC1 Loading	Cluster
Bridge Health Index (Overall)	0.549448	0
Bridge Health Index (Super)	0.468386	0
Bridge Health Index (Sub)	0.428205	0
Bridge Health Index (Deck)	0.409814	0
MIN_VERT_CLR_010	0.075473	0
MAX_SPAN_LEN_MT_048	0.049795	1
STRUCTURE_LEN_MT_049	0.505065	1
MAIN_UNIT_SPANS_045	0.405073	1
DECK_WIDTH_MT_052	0.315406	1
FUTURE_ADT_114	0.310284	1
Bridge Health Index (Overall)	0.491868	2
Bridge Health Index (Super)	0.434160	2
Bridge Health Index (Sub)	0.406215	2
Bridge Health Index (Deck)	0.344288	2
MIN_VERT_CLR_010	0.284759	2
STRUCTURE_LEN_MT_049	0.487836	3
DECK_AREA	0.487416	3
MAX_SPAN_LEN_MT_048	0.417833	3
MAIN_UNIT_SPANS_045	0.326119	3
SERVICE_ON_042A	0.324725	3
Bridge Health Index (Overall)	0.439393	4
Bridge Health Index (Deck)	0.344630	4
Bridge Health Index (Super)	0.313949	4
FUTURE_ADT_114	0.252962	4
Bridge Health Index (Sub)	0.227764	4
FUTURE_ADT_114	0.440412	5
MAX_SPAN_LEN_MT_048	0.374116	5
PIER_PROTECTION_111	0.369821	5
PERCENT_ADT_TRUCK_109	0.345292	5
SERVICE_ON_042A	0.336789	5

Cluster 5 bridges are characterized by high projected traffic demand, large span capacity, and design for resilience. Key PC1 contributors, future ADT, span length, pier protection, and truck percentage reflect their role in supporting commercial traffic and structural endurance. Moderate loadings from service type, reconstruction year, and deck condition point to partial upgrades and strategic importance. While BHI scores are positive, they are not defining features. A strong negative loading from functional class suggests these bridges may serve less prominent roads despite their scale. Overall, Cluster 5 includes durable, long-span structures critical for connectivity but not always administratively prioritized.

3.1.3. Key Observations

The cluster analysis revealed a wide range of long-term deterioration trajectories with meaningful implications for asset management. While all six groups differ in the magnitude and pace of deterioration, they also vary in how they respond to intervention highlighting

the strategic role of preventive maintenance and timely rehabilitation. Preventive maintenance is most evident in Cluster 0, where bridges maintained consistently high BHI values (≈95–97) over nearly three decades. Their narrow uncertainty bands and supportive PCA loadings indicate stable performance driven by routine attention. Although these bridges are generally smaller and lower-traffic, their sustained condition illustrates the long-term value of systematic preventive care. Clusters 2 and 3 illustrate the benefits of rehabilitation. Cluster 2 bridges, which began in poor condition (median ≈ 50), experienced rapid improvement following intervention, stabilizing above 90 thereafter. Cluster 3 shows a U-shaped pattern with decline followed by recovery and long-term stabilization. While this trajectory is interpreted as rehabilitation-driven, we note that this is an inference based on trend shape rather than confirmed maintenance records. These clusters highlight how targeted mid-life rehabilitation can reverse deterioration and extend service life. Cluster 1 shows gradual decline among larger, higher-traffic bridges moving from ≈90 to ≈85 with widening uncertainty bands. PCA loadings indicate aging without commensurate maintenance response. Though not yet critical, these bridges require targeted monitoring and scheduled intervention to avoid escalation. Cluster 4 represents moderate, steady decline (≈from 90 to 70) and limited evidence of recent intervention. Its trend suggests missed rehabilitation opportunity, though capacity remains recoverable if action is taken soon. Cluster 5 exhibits severe deterioration, with BHI collapsing from above 80 to below 20 in only a few years, accompanied by wide uncertainty bands during decline. These bridges are large, high-traffic assets whose rapid failure signals urgent need for inspection and remediation. Across clusters, the results reinforce how maintenance strategies, not merely aging, drives long-term outcomes. Preventive care supports stable trajectories, timely rehabilitation drives recovery, and deferred action corresponds to decline. The cluster framework therefore provides a practical tool for benchmarking performance and prioritizing interventions across the network.

This uncertainty analysis not only validates the robustness of observed trends but also helps prioritize interventions where variability signals emerging risks.

Table 21 presents the RMSE results across the steel bridge clusters. Clusters 0 and 1 exhibit low RMSEs (2.69 and 4.03, respectively) with large sample sizes, indicating stable and representative deterioration patterns. In contrast, Clusters 2 through 5 show higher RMSEs (ranging from 10.83 to 22.66) and smaller bridge counts, reflecting more diverse or less stable behavior. Overall, these findings highlight that lower RMSEs and larger cluster sizes correspond to more reliable deterioration patterns, whereas higher RMSEs in sparse clusters require more cautious interpretation.

Table 21. Root Mean Squared Error (RMSE) Summary for Steel Bridge Clusters.

Bridge Type	Cluster	RMSE	Number of Bridges in Clusters
Steel	0	2.69	757
Steel	1	4.03	503
Steel	2	14.70	35
Steel	3	13.36	33
Steel	4	10.83	44
Steel	5	22.66	6

From an engineering and policy perspective, these RMSE-based stability measures provide a practical way to distinguish reliable cluster patterns from outliers, reducing the risk of basing interventions on spurious trends. This moves beyond regression-based approaches [17,60,61], which struggled with small datasets and could obscure heterogeneous outcomes. For policymakers, this means that funding can be more confidently directed to clusters with proven, stable deterioration patterns, while unstable or sparsely populated

groups are flagged for further data collection before investment decisions are made. These findings reinforce the value of clustering-based analysis for infrastructure planning and performance monitoring. By grouping bridges based on shared deterioration trajectories and structural characteristics, transportation agencies can move beyond reactive maintenance and adopt a more proactive, data-driven approach. This method allows for early identification of at-risk structures and prioritization of resource allocation based on empirical patterns rather than isolated assessments. In particular, Clusters 3 and 5 among steel bridges illustrate how early declines, when followed by effective interventions, can stabilize performance or, when neglected, can lead to sustained degradation. These cases highlight the potential benefits of early rehabilitation and targeted inspection policies. When integrated with measures such as RMSE-based stability assessments and material-specific trend patterns, this clustering framework offers a scalable and interpretable strategy for statewide asset management and long-term resilience planning. Compared with previous deterioration studies that reported largely linear or monotonic aging trends across bridge types [62,63], our findings show that deterioration is rarely uniform. Instead, bridges often exhibit nonlinear patterns of decline, stabilization, and recovery, shaped by both material properties and intervention history [17,64]. This comparative insight underscores the value of clustering for uncovering diverse deterioration archetypes that average-based models cannot capture [18].

3.2. Practical Implications

The findings of this study present important implications for infrastructure planning and asset management, particularly for agencies like the Maryland Department of Transportation (MDOT) and other state-level Departments of Transportation (DOTs) seeking to transition toward more data-driven decision-making frameworks. By uncovering latent deterioration patterns through time-series clustering and Principal Component Analysis (PCA), this analysis offers a new lens through which bridge performance can be assessed not solely as isolated structures but as components of broader deterioration archetypes. Critically, the clusters identified across Maryland's steel bridge network reflect not only differences in condition levels but also in the underlying mechanisms of deterioration. For example, Cluster 0 bridges, with consistently high BHI scores and minimal geometric complexity, suggest a stable cohort benefiting from either favorable design features, lower stress environments, or consistent preventive maintenance. In contrast, Cluster 5 bridges with sharply declining BHI values and high projected traffic demand reveal the consequences of sustained neglect or insufficient intervention in high-risk contexts. These patterns do more than illustrate variation; they signal where and why deterioration is occurring, and what that implies for future performance if left unaddressed.

Because the sample sizes of Clusters 2–5 are small, the higher RMSE values and wider confidence intervals reported for these groups reflect greater uncertainty, and conclusions for these clusters should be interpreted carefully. In addition, annual BHI records produce short trajectories for each bridge, which means that quantitative symmetry indices (such as pre- vs. post-minimum slope ratios or deviation-based symmetry scores) were not applied to avoid over-interpreting low-resolution data. We identify the development of symmetry metrics using higher-frequency inspection records as an important direction for future work.

The integration of PCA reinforces these interpretations by linking deterioration trends to structural and operational attributes. For instance, high loadings for span length and future traffic in Cluster 1 suggest that size and usage intensity are critical stressors contributing to gradual decline. The negative loadings for BHI metrics within the same cluster further underscore the structural toll of such demands, suggesting that existing inspection and maintenance regimes may not be fully aligned with the evolving stress profiles of these

assets. In this context, deterioration is not simply a function of time but of the interaction between design, demand, and deferred rehabilitation. These insights directly support the goals of Maryland's Bridge and Asset Management Program (BAMP), which seeks to align resource allocation with long-term performance outcomes. Rather than applying uniform inspection intervals across all assets, MDOT could use these cluster-based classifications to implement differentiated monitoring strategies. Stable bridges, such as those in Cluster 0, may warrant longer inspection cycles, reducing operational costs without compromising safety. Conversely, bridges exhibiting early-stage degradation (Cluster 3) or sustained critical decline (Cluster 5) could be flagged for accelerated inspection and targeted funding.

Moreover, these clusters provide a framework for understanding preventive action efficacy. Cluster 2, for example, shows a sharp improvement in BHI following early decline a trajectory likely resulting from timely rehabilitation. In contrast, the persistent low performance of Cluster 5 underscores the risks of delayed response. These comparative narratives offer powerful evidence for why early intervention matters, and how strategic reinvestment can alter the trajectory of bridge health. For MDOT and other DOTs, this substantiates a shift from reactive to anticipatory maintenance, where budget decisions are guided by deterioration risk rather than post-failure urgency. Finally, the interpretability of the cluster-PCA framework enhances its policy relevance. Clusters can be tied to specific bridge traits such as span length, traffic volume, age, reconstruction history allowing agencies to identify vulnerable typologies and allocate funding more equitably. This not only supports more effective maintenance prioritization but also facilitates transparent communication with stakeholders and policymakers, grounding infrastructure decisions in empirical patterns rather than ad hoc assessments. In sum, the clustering and PCA framework does not merely categorize bridges, it provides a strategic blueprint for infrastructure resilience. For MDOT and peer agencies, adopting such an approach could enable more precise targeting of limited resources, reduce lifecycle costs, and ensure the longevity and safety of critical transportation assets.

3.3. Limitations

While the clustering framework provides valuable insights into network-level deterioration trends, several limitations must be acknowledged. First, the analysis relies on the accuracy and consistency of Bridge Health Index (BHI) data, which may be affected by subjective condition assessments and inconsistencies in reporting across inspection cycles. In addition, some critical variables such as construction year or component-level attributes were missing for a subset of bridges or time periods, limiting the ability to fully contextualize deterioration patterns. The clustering results are also sensitive to preprocessing decisions, including the methods used for imputing missing values and the choice of distance metric. This study employed Euclidean distance for simplicity and interpretability, but alternative techniques such as dynamic time warping or probabilistic sequence models may better capture nonlinear or irregular trajectories and improve cluster alignment. Another limitation is the lack of access to detailed maintenance and rehabilitation records. While sudden changes in BHI trends may suggest intervention or failure events, without intervention logs these shifts cannot be definitively explained. Finally, the analysis was limited to Maryland's bridge inventory. While this enables actionable state-level recommendations, broader validation across multiple states and climates would strengthen generalizability. Together, these limitations highlight areas for future research and underscore the importance of improving data quality and availability to support more accurate and actionable infrastructure assessments.

4. Discussion

This study demonstrated that time-series clustering of Bridge Health Index (BHI) trajectories can effectively capture the diversity of deterioration behaviors within Maryland's steel bridge network. The six identified clusters reveal that deterioration is far from uniform bridges, following distinct trajectories of stability, decline, and recovery. These patterns highlight how maintenance strategy, environmental exposure, and usage intensity collectively shape long-term structural performance.

1. Stable clusters (Cluster 0) underscore the long-term benefits of preventive maintenance and consistent inspection practices.
2. Recovering clusters (2 and 3) confirm that rehabilitation interventions, even when delayed, can restore condition and prolong service life.
3. Declining clusters (1 and 4) reveal the effects of gradual wear, deferred maintenance, and increasing traffic demand.
4. Critically deteriorated bridges (Cluster 5) illustrate the structural and operational consequences of prolonged neglect, particularly in high-traffic corridors.

These patterns collectively demonstrate that deterioration is not purely a function of material aging but of management decisions, proactive care can stabilize decline, while deferred maintenance accelerates structural loss.

Compared with previous deterioration modeling approaches (Markov chains, regression-based forecasts), this study shows that clustering and PCA uncover nonlinear and recovery behaviors that traditional models often overlook. Past work, such as [29] and [30], similarly identified groups of bridges with shared aging profiles but did not incorporate continuous BHI trends or uncertainty quantification.

By contrast, the integration of bootstrap confidence intervals in this study adds statistical rigor, confirming that observed stability or deterioration is not a random artifact. Additionally, PCA-based feature interpretation distinguishes structural and contextual variables (span length, ADT, deck width) that drive these differences. This integrated framework therefore extends the literature by moving from descriptive clustering toward interpretable and confidence-based classification of deterioration behaviors.

From a management perspective, the cluster-PCA framework offers a scalable and interpretable tool for data-informed decision-making.

1. Inspection Scheduling: Stable clusters could justify longer inspection intervals, reducing costs without compromising safety.
2. Prioritization: Deteriorating and high-risk clusters (4 and 5) should be prioritized for detailed inspection, rehabilitation, or replacement.
3. Budget Allocation: Cluster-level trends allow agencies such as MDOT to link funding priorities to quantifiable deterioration archetypes.
4. Performance Benchmarking: Stable and recovering clusters can serve as benchmarks for best maintenance practices and lifecycle cost optimization.

These findings align with the goals of Maryland's Bridge and Asset Management Program (BAMP) and provide a framework for shifting from reactive to preventive infrastructure management.

This study introduces a novel integration of time-series clustering, bootstrap-based uncertainty analysis, and PCA-driven feature interpretation. This combination enables:

1. Detection of shared deterioration trajectories at the network scale,
2. Quantification of confidence in observed trends
3. Interpretation of structural and contextual drivers of deterioration.

Such integration bridges the gap between statistical rigor and engineering interpretability, demonstrating how unsupervised learning can complement existing Bridge Management Systems (BMS).

Although the deterioration archetypes identified in this study are specific to Maryland's climatic and operational environment, the analytical methodology is broadly generalizable. The preprocessing pipeline, z-score normalization, K-means clustering, bootstrap uncertainty quantification, and PCA interpretation procedures operate on standardized numerical inputs and can be directly applied to comparable condition datasets in other regions. Thus, the framework introduced here is scalable and transferable, enabling transportation agencies to uncover context-dependent deterioration patterns in their own bridge networks.

5. Conclusions

This study presented a comprehensive, data-driven evaluation of long-term deterioration behavior across Maryland's steel bridges using Bridge Health Index (BHI) time-series clustering, bootstrap uncertainty quantification, and Principal Component Analysis (PCA). The approach revealed substantial variation in structural performance trajectories and enabled a rigorous interpretation of the underlying characteristics that drive deterioration patterns.

Key Findings

1. Six deterioration archetypes were identified, reflecting stable, declining, recovering, and severely deteriorating long-term performance behaviors across Maryland's steel bridges;
2. Cluster 0 bridges exhibited persistently high BHI values over nearly three decades, with narrow confidence intervals confirming long-term structural stability;
3. Clusters 1 and 4 showed sustained decline, with PCA indicating that large geometry, higher traffic demand, and aging correspond to downward trends and C
4. Clusters 2 and 3 displayed recovery or U-shaped trajectories, suggesting the influence of rehabilitation or maintenance interventions reflected by narrowing uncertainty bands;
5. Cluster 5 demonstrated pronounced, persistent deterioration, with wide uncertainty early in the time series converging to critically low BHI values in recent years;
6. Cluster-wise PCA confirmed distinct structural and operational drivers of deterioration, such as span length, deck area, truck percentage, and BHI component values;
7. Bootstrap confidence intervals validated the robustness of cluster-level median trajectories and PCA interpretations, while highlighting uncertainty in smaller clusters.

Significance of the Study

1. Establishes a reproducible methodology for large-scale deterioration trajectory modeling;
2. Demonstrates how clustering, bootstrap confidence intervals, and PCA can distinguish systematic degradation from random variation;
3. Provides a scalable diagnostic tool to support proactive, targeted maintenance strategies and inspection prioritization;
4. Highlights the importance of considering structural context, operational exposure, and intervention timing not just age or material.

Limitations

1. Absence of maintenance, rehabilitation, and repair records limits the causal attribution of sudden BHI changes;
2. Small cluster membership (n = 6) increases uncertainty and limits generalizability for sparse groups.

Future Research Directions

1. Integrate detailed MDOT maintenance and rehabilitation logs to validate inferred deterioration mechanisms;
2. Expand sensitivity testing using alternative similarity metrics (DTW), probabilistic clustering, and hybrid models;
3. Incorporate environmental exposure, climate stressors, and traffic growth projections to support scenario-based forecasting;
4. Implement the framework within real-time infrastructure management systems for adaptive inspection scheduling;
5. Evaluate the generalizability of deterioration archetypes using bridge networks in different climatic or operational contexts.

Overall, this study introduces a rigorous, scalable analytical framework that enhances the precision and interpretability of deterioration modeling and offers actionable insights for long-term bridge asset management.

Author Contributions: Conceptualization, M.S.; methodology, S.P. and Z.B.; software, S.P.; model development, S.P.; validation, M.S., Z.B., S.P. and R.S.; formal analysis, S.P.; Investigation M.S.; resources, R.S.; data curation, S.P.; writing—original draft preparation, S.P.; writing—review and editing, M.S. and Z.B.; visualization, S.P.; supervision, M.S.; project administration, M.S.; funding acquisition, M.S. The study was initiated by M.S., who also played a crucial role in validating the results and refining the methodology. All authors have read and agreed to the published version of the manuscript.

Funding: This research was funded by the Center for Integrated Asset Management for Multimodal Transportation Infrastructure Systems (CIAMTIS). We are grateful for their support, which was crucial in enabling this research.

Data Availability Statement: The data supporting the findings of this study are openly available, in accordance with MDPI's data-sharing policies. The dataset has been organized into a publicly accessible Google document, which can be shared upon request to ensure the transparency and reproducibility of the research results. Interested researchers may contact the corresponding author to gain access to the data. No new data were created during this study; the analysis is based on pre-existing data that adhere to privacy and ethical standards.

Acknowledgments: During the preparation of this manuscript, the authors used *ChatGPT* (*OpenAI*, *GPT-5*) and *Grammarly Premium* for the purposes of improving grammar, spelling, punctuation, and overall language clarity. The authors have reviewed and edited the output and take full responsibility for the content of this publication. This statement is provided for transparency.

Conflicts of Interest: The authors declare no conflicts of interest. The funders had no role in the design of the study; in the collection, analyses, or interpretation of data; in the writing of the manuscript; or in the decision to publish the results.

Abbreviations

The following abbreviations are used in this manuscript:

BHI	Bridge Health Index
PCA	Principal Component Analysis
FHWA	Federal Highway Administration
MDOT	Maryland Department of Transportation
BMS	Bridge Management Systems
NBI	National Bridge Inventory
NCDOT	North Carolina Department of Transportation

DLUHS	Deep Learning–based Uniform Hazard Spectral acceleration
SHM	Structural Health Monitoring
GMM	Gaussian Mixture Model
t-SNE	t-Distributed Stochastic Neighbor Embedding
SNOB	Sequential Number and Object Bayesian classifier
ROC	Receiver Operating Characteristic
AUC	Area Under the Curve
DBSCAN	Density-Based Spatial Clustering of Applications with Noise
GNSS	Global Navigation Satellite System
MDTA	Maryland Transportation Authority
DBHI	Denver Bridge Health Index
MPCA	Multilinear Principal Component Analysis
KNN	K-Nearest Neighbors
PC1	Principal Component 1
NOAA	National Oceanic and Atmospheric Administration
ADT	Average Daily Traffic
RMSE	Root Mean Square Error
CI/CIs	Confidence Interval(s)
BAMP	Bridge and Asset Management Program
DOT/DOTs	Department(s) of Transportation

References

1. American Society of Civil Engineers. A Comprehensive Assessment of America's Infrastructure. 2025. Available online: https://infrastructurereportcard.org/wp-content/uploads/2025/03/Full-Report-2025-Natl-IRC-WEB.pdf (accessed on 24 July 2025).
2. American Road & Transportation Builders Association. Bridge Report. 2024. Available online: https://artbabridgereport.org/reports/2024-ARTBA-Bridge-Report.pdf (accessed on 24 July 2025).
3. Brent Spence Bridge Corridor Project and Virginia Department of Transportation. Bridges. 2025. Available online: https://infrastructurereportcard.org/wp-content/uploads/2025/03/Bridges.pdf (accessed on 24 July 2025).
4. Wlaschin, J.B.; Miller, H. *Management Systems: Driving Performance a Glance at Data-Driven Decisionmaking Practices*; U.S. Department of Transportation/Federal Highway Administration: Washington, DC, USA, 2009.
5. Gee, K.W.; Henderson, G. Highway Bridge Inspections | US Department of Transportation. Available online: https://www.transportation.gov/testimony/highway-bridge-inspections (accessed on 24 July 2025).
6. Moore, M.; Phares, B.M.; Graybeal, B.; Rolander, D.; Washer, G.; Wiss, J. Reliability of Visual Inspection for Highway Bridges, Volume I: Final Report. 2001. Available online: https://www.fhwa.dot.gov/publications/research/nde/pdfs/01020a.pdf (accessed on 28 November 2025).
7. Kong, X.; Liu, Z.; Liu, H.; Hu, J.; Deng, L. Recent advances on inspection, monitoring, and assessment of bridge cables. *Autom. Constr.* **2024**, *168*, 105767. [CrossRef]
8. American Road & Transportation Builders Association. National Bridge Inventory: Maryland. 2024. Available online: https://artbabridgereport.org/economic-reports/export-pdf?state=MD (accessed on 24 July 2025).
9. FHWA. Bridge Condition by Highway System. Available online: https://www.fhwa.dot.gov/Bridge/nbi/no10/condition24.cfm (accessed on 24 July 2025).
10. KCI Technologies, Inc. & TranSystems. Maryland SHA Management Plan for Historic Highway Bridges. 2012. Available online: https://roads.maryland.gov/OPPEN/Maryland%20SHA%20Management%20Plan%20for%20Historic%20Highway%20Bridges.pdf (accessed on 17 September 2025).
11. Maryland Department of Transportation. Asset Management Plan. 2021. Available online: https://www.mdot.maryland.gov/OPCP/MDOT_AMP_EF_2021_06_03.pdf (accessed on 24 July 2025).
12. Mohammadagha, M.; Najafi, M.; Kaushal, V.; Jibreen, A.M.A. Machine Learning Models for Reinforced Concrete Pipes Condition Prediction: The State-of-the-Art Using Artificial Neural Networks and Multiple Linear Regression in a Wisconsin Case Study. *arXiv* **2025**. [CrossRef]
13. Hasan, M.S. Deterioration Prediction of Concrete Bridge Components Using Artificial Intelligence and Stochastic Methods. 2015. Available online: https://research-repository.rmit.edu.au/articles/thesis/Deterioration_prediction_of_concrete_bridge_components_using_artificial_intelligence_and_stochastic_methods/27591186?file=50761449 (accessed on 28 November 2025).

14. Stevens, N.-A.; Lydon, M.; Marshall, A.H.; Taylor, S. Identification of Bridge Key Performance Indicators Using Survival Analysis for Future Network-Wide Structural Health Monitoring. *Sensors* **2020**, *20*, 6894. [CrossRef] [PubMed]
15. Cavalline, T.L.; Whelan, M.J.; Tempest, B.Q.; Goyal, R.; Ramsey, J.D. Determination of Bridge Deterioration Models and Bridge User Costs for the NCDOT Bridge Management System. 2015. Available online: https://connect.ncdot.gov/projects/research/RNAProjDocs/2014-07FinalReport.pdf (accessed on 24 July 2025).
16. Feng, G. (Ed.) *Proceedings of the 10th International Conference on Civil Engineering*; Lecture Notes in Civil Engineering; Springer Nature: Singapore, 2024. [CrossRef]
17. Lamei, T.; Abdel-Rahim, A.; Ibrahim, A. Development of performance-based deterioration models for bridge components. *Innov. Infrastruct. Solut.* **2025**, *10*, 230. [CrossRef]
18. Faris, N.; Zayed, T.; Fares, A. Review of Condition Rating and Deterioration Modeling Approaches for Concrete Bridges. *Buildings* **2025**, *15*, 219. [CrossRef]
19. Anderson, J.C.; Unnikrishnan, A.; Schumacher, T. Heterogeneity-Based Survival Analysis of NBI Condition Ratings for Concrete Highway Bridge Decks in Oregon by Condition Group. 2021. Available online: https://ascelibrary.org/doi/10.1061/(ASCE)IS.1943-555X.0000636 (accessed on 24 July 2025).
20. Illinois Institute of Technology; Fu, G. *Evaluation of Illinois Bridge Deterioration Models*; Illinois Center for Transportation: Rantoul, IL, USA, 2021. [CrossRef]
21. Goyal, R. *Bridge Condition Rating Forecast—Survival-Based Models*; Federal Highway Administration: Washington, DC, USA, 2020.
22. Gatesi, J.D.D.; Chingui, J.A.; Botir, E. A Review of Bridge Management System: Deterioration Models. *Asian J. Eng. Technol.* **2020**, *8*, 75824083. [CrossRef]
23. Shokrgozar-Yatimdar, E.; Chen, P. Explainable deep learning for real-time prediction of uniform hazard spectral acceleration for on-site earthquake early warning. *Geophys. J. Int.* **2025**, *243*, ggaf345. [CrossRef]
24. Masiero, A.; Guarnieri, A.; Baiocchi, V.; Visintini, D.; Pirotti, F. Machine Learning Clustering Techniques to Support Structural Monitoring of the Valgadena Bridge Viaduct (Italy). *Remote Sens.* **2024**, *16*, 3971. [CrossRef]
25. Shahrivar, F.; Sidiq, A.; Mahmoodian, M.; Jayasinghe, S.; Sun, Z.; Setunge, S. AI-based bridge maintenance management: A comprehensive review. *Artif. Intell. Rev.* **2025**, *58*, 135. [CrossRef]
26. Plevris, V.; Papazafeiropoulos, G. AI in Structural Health Monitoring for Infrastructure Maintenance and Safety. *Infrastructures* **2024**, *9*, 225. [CrossRef]
27. Coraça, E.M.; Ferreira, J.V.; Nóbrega, E.G.O. An unsupervised structural health monitoring framework based on Variational Autoencoders and Hidden Markov Models. *Reliab. Eng. Syst. Saf.* **2023**, *231*, 109025. [CrossRef]
28. Eltouny, K.; Gomaa, M.; Liang, X. Unsupervised Learning Methods for Data-Driven Vibration-Based Structural Health Monitoring: A Review. *Sensors* **2023**, *23*, 3290. [CrossRef] [PubMed]
29. Landi, F.; Marsili, F.; Keßler, S.; Croce, P. An unsupervised learning approach to predict the deterioration of aging bridges using inspection data. *Struct. Concr.* **2025**, *26*, 5454–5468. [CrossRef]
30. Chang, K.; Chi, S. Bridge Clustering for Systematic Recognition of Damage Patterns on Bridge Elements. *J. Comput. Civ. Eng.* **2019**, *33*, 04019028. [CrossRef]
31. Chen, B.; Zhang, J.; Wang, Y. Principal Component Stochastic Subspace Identification for Output-Only Modal Analysis. *arXiv* **2025**, arXiv:2504.00317. [CrossRef]
32. Hurtado, A.C.; Alamdari, M.M.; Atroshchenko, E.; Chang, K.C.; Kim, C.W. A data-driven methodology for bridge indirect health monitoring using unsupervised computer vision. *Mech. Syst. Signal Process.* **2024**, *210*, 111109. [CrossRef]
33. Zhou, L.; Lai, P.; Zhao, W.; Yang, Y.; Shi, A.; Li, X.; Ma, J. A Noise Reduction Method for GB-RAR Bridge Monitoring Data Based on CEEMD-WTD and PCA. *Symmetry* **2025**, *17*, 588. [CrossRef]
34. Zunino, L.; Casas, J.R.; Domaneschi, M. Bridge damage assessment under traffic and environmental variability: A case study on Yonghe cable-stayed bridge. *Eng. Struct.* **2025**, *343*, 120965. [CrossRef]
35. Abdullah, H.A.; Hanif, M.U.; Hassan, M.U.; Shahid, J.M.; Khan, S.A.; Ali, A. Improved damage assessment of bridges using advanced signal processing techniques of CEEMDAN-EWT and Kernal PCA. *Eng. Struct.* **2025**, *329*, 119774. [CrossRef]
36. Brighenti, F.; Caspani, V.F.; Costa, G.; Giordano, P.F.; Limongelli, M.P.; Zonta, D. Bridge management systems: A review on current practice in a digitizing world. *Eng. Struct.* **2024**, *321*, 118971. [CrossRef]
37. Buckley, T.; Ghosh, B.; Pakrashi, V. A Feature Extraction & Selection Benchmark for Structural Health Monitoring. *Struct. Health Monit.* **2022**, *22*, 2082–2127. [CrossRef]
38. Li, Z.; Lan, Y.; Lin, W. Investigation of Frequency-Domain Dimension Reduction for A2M-Based Bridge Damage Detection Using Accelerations of Moving Vehicles. *Materials* **2023**, *16*, 1872. [CrossRef] [PubMed]
39. Neumann, L.; Wittenberg, P.; Mendler, A.; Gertheiss, J. Confounder-adjusted Covariances of System Outputs and Applications to Structural Health Monitoring. *arXiv* **2024**, arXiv:2409.17735. [CrossRef]
40. Xia, Y.; Lei, X.; Wang, P.; Sun, L. A data-driven approach for regional bridge condition assessment using inspection reports. *Struct. Control Health Monit.* **2021**, *29*, e2915. [CrossRef]

41. Ma, Y.; Liu, X.; Wang, B.; Liu, Y. Intelligent Diagnosis of Highway Bridge Technical Condition Based on Defect Information. *Struct. Durab. Health Monit.* **2024**, *18*, 871–889. [CrossRef]
42. Sen, D.; Erazo, K.; Zhang, W.; Nagarajaiah, S.; Sun, L. On the effectiveness of principal component analysis for decoupling structural damage and environmental effects in bridge structures. *J. Sound Vib.* **2019**, *457*, 280–298. [CrossRef]
43. Yuan, Y.; Zhu, X.; Li, J. Moving-Principal-Component-Analysis-Based Structural Damage Detection for Highway Bridges in Operational Environments. *Sensors* **2024**, *24*, 383. [CrossRef] [PubMed]
44. Pan, J.; Wang, X.; Huang, K.; Wang, W. Symmetrically Construction Monitoring Analysis and Completed State Evaluation of a Tied Steel Box Arch Bridge Based on Finite Element Method. *Symmetry* **2023**, *15*, 932. [CrossRef]
45. Yang, Y. Symmetry in Safety and Disaster Prevention Engineering. *Symmetry* **2023**, *15*, 2101. [CrossRef]
46. Farhey, D.N. Reconstruction as Deterioration Indicator for Operational Structural Performances of Bridge Materials. *Infrastructures* **2022**, *7*, 96. [CrossRef]
47. Dizaj, E.A.; Salami, M.R.; Kashani, M.M. Impact of asymmetrical corrosion of piers on seismic fragility of ageing irregular concrete bridges. *Struct. Infrastruct. Eng.* **2025**, *21*, 1465–1484. [CrossRef]
48. FHWA. *FHWA Bridge Preservation Research Roadmap*; FHWA-HRT-24-011; FHWA: Washington, DC, USA, 2024.
49. U.S. Department of Transportation. Bridge Preservation Guide. 2018. Available online: https://www.fhwa.dot.gov/bridge/preservation/guide/guide.pdf (accessed on 24 July 2025).
50. Scherr, J.F.; Grosse, C.U.; Popovics, J.S. Evaluation of non-destructive impact-echo data from the national bridge inventory. *Dev. Built Environ.* **2024**, *18*, 100468. [CrossRef]
51. Din, Z.U.; Tang, P. Automatic Logical Inconsistency Detection in the National Bridge Inventory. *Procedia Eng.* **2016**, *145*, 729–737. [CrossRef]
52. Sanford, K.L.; Herabat, P.; Mcneil, S. Bridge Management and Inspection Data: Leveraging the Data and Identifying the Gaps. In Proceedings of the 8th International Bridge Management Conference, Barcelona, Spain, 18–22 July 2022.
53. Karaaslan, E.; Bagci, U.; Catbas, N. A Novel Decision Support System for Long-Term Management of Bridge Networks. *Appl. Sci.* **2021**, *11*, 5928. [CrossRef]
54. Hanley, C.; Kelliher, D.; Pakrashi, V. Principal Component Analysis for Condition Monitoring of a Network of Bridge Structures. *J. Phys. Conf. Ser.* **2015**, *628*, 012060. [CrossRef]
55. Wang, X.; Gao, Q.; Liu, Y. Damage Detection of Bridges under Environmental Temperature Changes Using a Hybrid Method. *Sensors* **2020**, *20*, 3999. [CrossRef] [PubMed]
56. Sonbul, O.; Rashid, M. Algorithms and Techniques for the Structural Health Monitoring of Bridges: Systematic Literature Review. *Sensors* **2023**, *23*, 4230. [CrossRef]
57. Rizzo, P.; Enshaeian, A. Challenges in Bridge Health Monitoring: A Review. *Sensors* **2021**, *21*, 4336. [CrossRef]
58. Xu, D.; Xu, X.; Forde, M.C.; Caballero, A. Concrete and steel bridge Structural Health Monitoring—Insight into choices for machine learning applications. *Constr. Build. Mater.* **2023**, *402*, 132596. [CrossRef]
59. Foster, D. *Bridge Deterioration Models and Rates*; Caltrans Division of Research, Innovation and System Information, Office of Asset Management: Sacramento, CA, USA, 2020.
60. Abdelkader, E.M.; Al-Sakkaf, A.; Elkabalawy, M.; Omar, A.; Alfalah, G. Simulating the Deterioration Behavior of Tunnel Elements Using Amalgamation of Regression Trees and State-of-the-Art Metaheuristics. *Mathematics* **2025**, *13*, 1021. [CrossRef]
61. Prakash, G.; Yuan, X.-X.; Hazra, B.; Mizutani, D. Toward a Big Data-Based Approach: A Review on Degradation Models for Prognosis of Critical Infrastructure. *ASME J. Nondestruct. Eval.* **2020**, *4*, 021005. [CrossRef]
62. Chase, S.B.; Small, E.P.; Nutakor, C. An In-Depth Analysis of the National Bridge Inventory Database Utilizing Data Mining, GIS and Advanced Statistical Methods. *Transp. Res. Circ.* **1999**, *498*, 1–17.
63. Srikanth, I.; Arockiasamy, M. Deterioration models for prediction of remaining useful life of timber and concrete bridges: A review. *J. Traffic Transp. Eng.* **2020**, *7*, 152–173. (In English) [CrossRef]
64. Fick, D.; Bell, M. *Western Transportation Institute. Development of Deterioration Curves for Bridge Elements in Montana*; Research Programs; Montana Department of Transportation: Bozeman, MT, USA, 2022. [CrossRef]

Disclaimer/Publisher's Note: The statements, opinions and data contained in all publications are solely those of the individual author(s) and contributor(s) and not of MDPI and/or the editor(s). MDPI and/or the editor(s) disclaim responsibility for any injury to people or property resulting from any ideas, methods, instructions or products referred to in the content.